École Doctorale des Sciences de l'Environnement d'Île-de-France
Année Universitaire 2024-2025

Modélisation Numérique de l'Écoulement Atmosphérique et Assimilation de Données

Olivier Talagrand
Cours 2

11 Avril 2025

Physical laws governing the flow

- Conservation of mass

  $D\rho/Dt + \rho \, \mathrm{div}\underline{U} = 0$

- Conservation of energy

  $De/Dt - (p/\rho^2) \, D\rho/Dt = Q$

- Conservation of momentum

  $D\underline{U}/Dt + (1/\rho) \, \underline{\mathrm{grad}}p - \underline{g} + 2 \, \underline{\Omega} \wedge \underline{U} = \underline{F}$

- Equation of state

  $f(p, \rho, e) = 0$ $\qquad\qquad (p/\rho = rT, \; e = C_v T)$

- Conservation of mass of secondary components (water in the atmosphere, salt in the ocean, chemical species, …)

  $Dq/Dt + q \, \mathrm{div}\underline{U} = S$

These physical laws must be expressed in practice in discretized (and necessarily imperfect) form, both in space and time

The climate system is a heat engine, which produces mechanical motion from heat (efficiency of about 7%).

Equations above are partial differential equations involving derivatives with respect to spatial and temporal coordinates, but they express physical laws that apply to finite masses or volumes (the basis of discretization in finite elements)

Geostrophic balance

In midlatitudes, and in both the atmosphere and the ocean, the horizontal components of the Coriolis acceleration and of the pressure gradient force are in approximate balance ($\approx$ 10% accuracy)

Large-scale Numerical Weather Prediction is based on the *primitive equations*, themselves based on a number of simplifications, and particularly the hydrostatic approximation

Climatic simulations are also built on primitive equations, and contain a much more detailed description of the oceanic circulation.

More costly nonhydrostatic models are used for small scale meteorology, and are being developed for global modeling.

- Numerical Weather Prediction. Present performance (mostly ECMWF)

- The meteorological observation system

- The problem of ‘Assimilation’

- Inverse Problems. Bayesian Estimation

- European Centre for Medium-Range Weather Forecasts (ECMWF)

- Centre européen pour les prévisions météorologiques à moyen terme (CEPMMT)

- Europäisches Zentrum für mittelfristige Wettervorhersage (EZMW)

As of 2025, 23 member states, 12 co-operating states

ECMWF established in 1975. Has produced daily forecasts since 1980

Headquarters in Reading (UK), Data Centre in Bologna (Italy)

ECMWF hosts part EU's Earth Observation *Copernicus* programme. That part has moved to Bonn (Germany)

Centre Européen pour les Prévisions Météorologiques à Moyen Terme (CEPMMT, Reading, GB)

Modèle IFS-HRES (Integrated Forecasting System – High Resolution).
Depuis mars 2016 :

Modèle hydrostatique, semi-spectral. Troncature triangulaire TCO1279 / O1280 (résolution horizontale ≈ 9 kilomètres)

137 niveaux dans la direction verticale (0 - 80 km)

Discrétisation en éléments finis dans la direction verticale (coordonnée hybride)

Dimension du vecteur d'état correspondant > 10^9

Pas de discrétisation temporelle (schéma semi-Lagrangien semi-implicite): 450 secondes

Intégré 2 fois par jour (00 et 12 UTC) à une échéance de 10 jours

Base time: Tue 01 Apr 2025 00 UTC Valid time: Thu 10 Apr 2025 00 UTC (+216h) Area : Europe

ECMWF

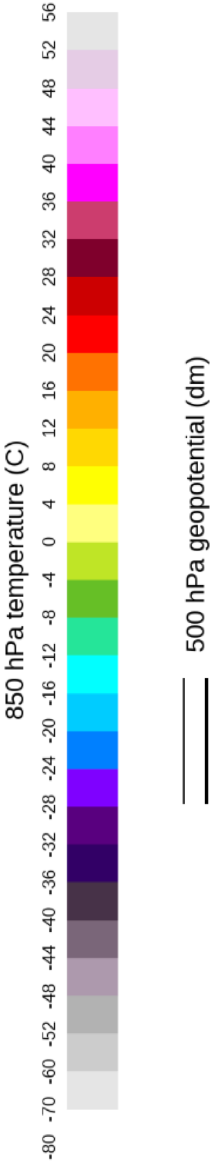

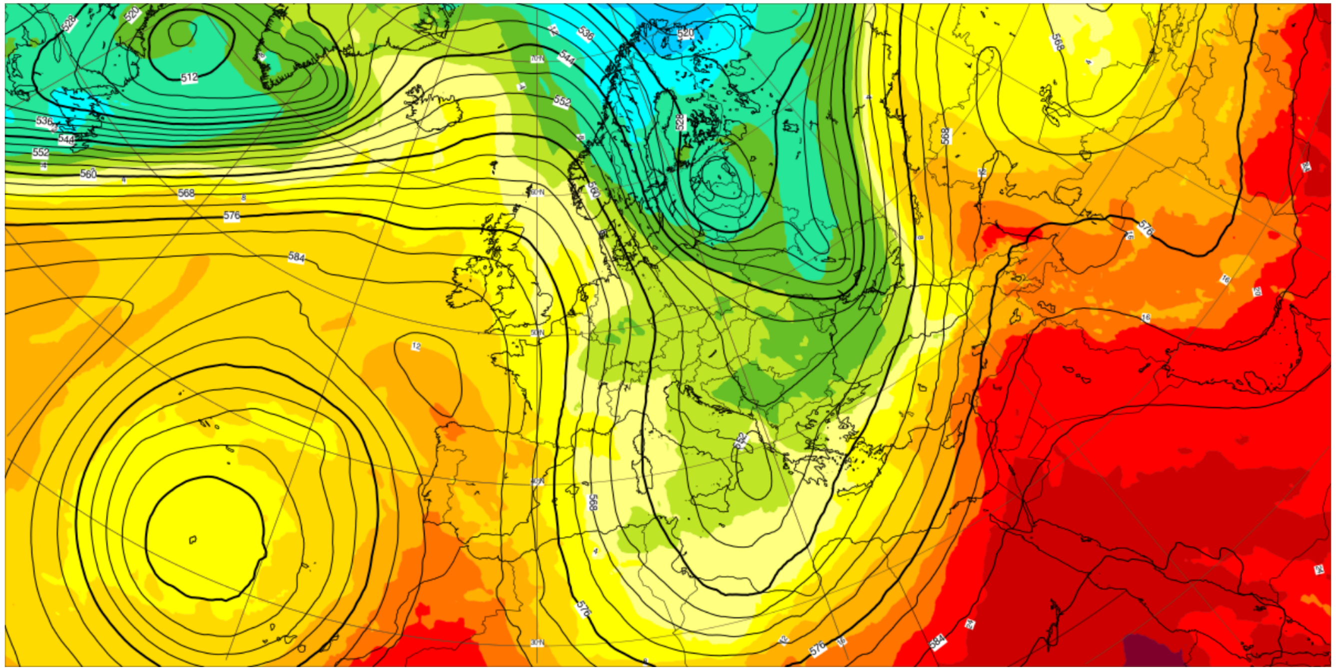

Base time: Thu 10 Apr 2025 00 UTC Valid time: Thu 10 Apr 2025 00 UTC (+0h) Area : Europe

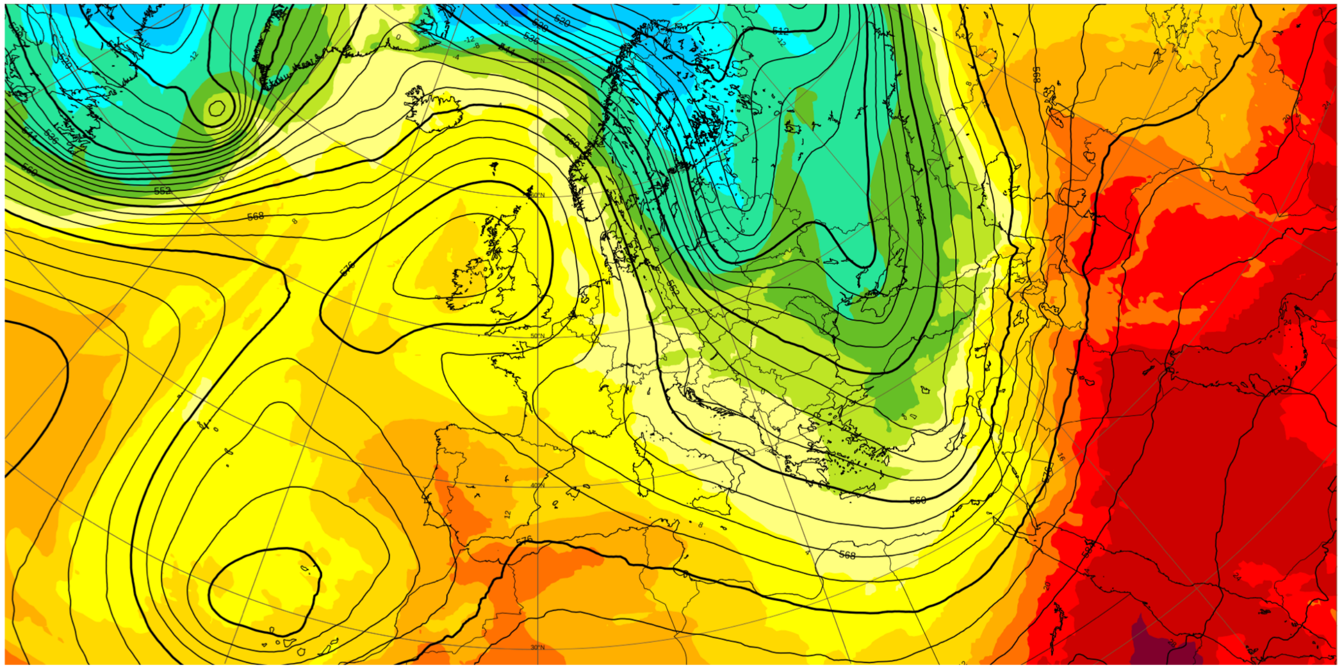

ECMWF

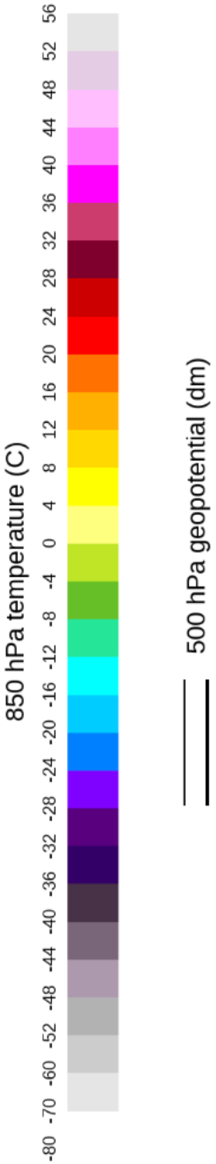

Base time: Tue 01 Apr 2025 00 UTC Valid time: Tue 01 Apr 2025 00 UTC (+0h) Area : Europe

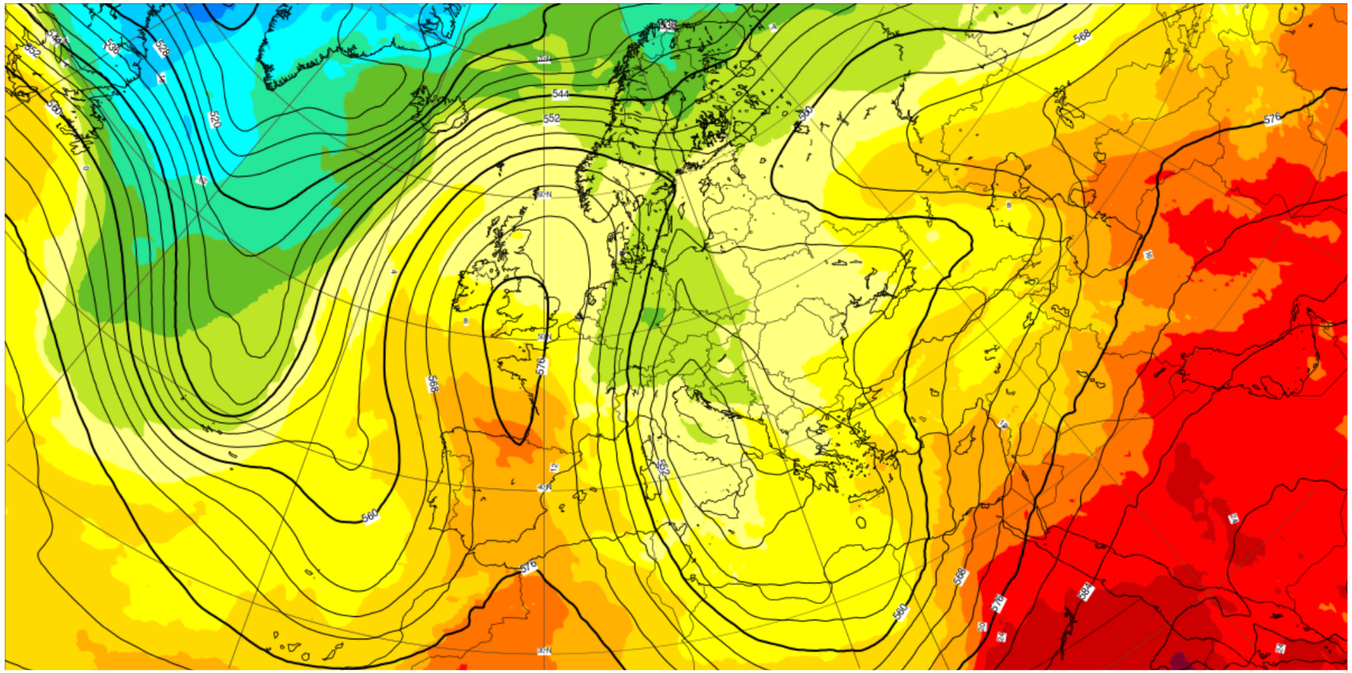

Base time: Thu 10 Apr 2025 00 UTC Valid time: Thu 10 Apr 2025 00 UTC (+0h) Area : Europe

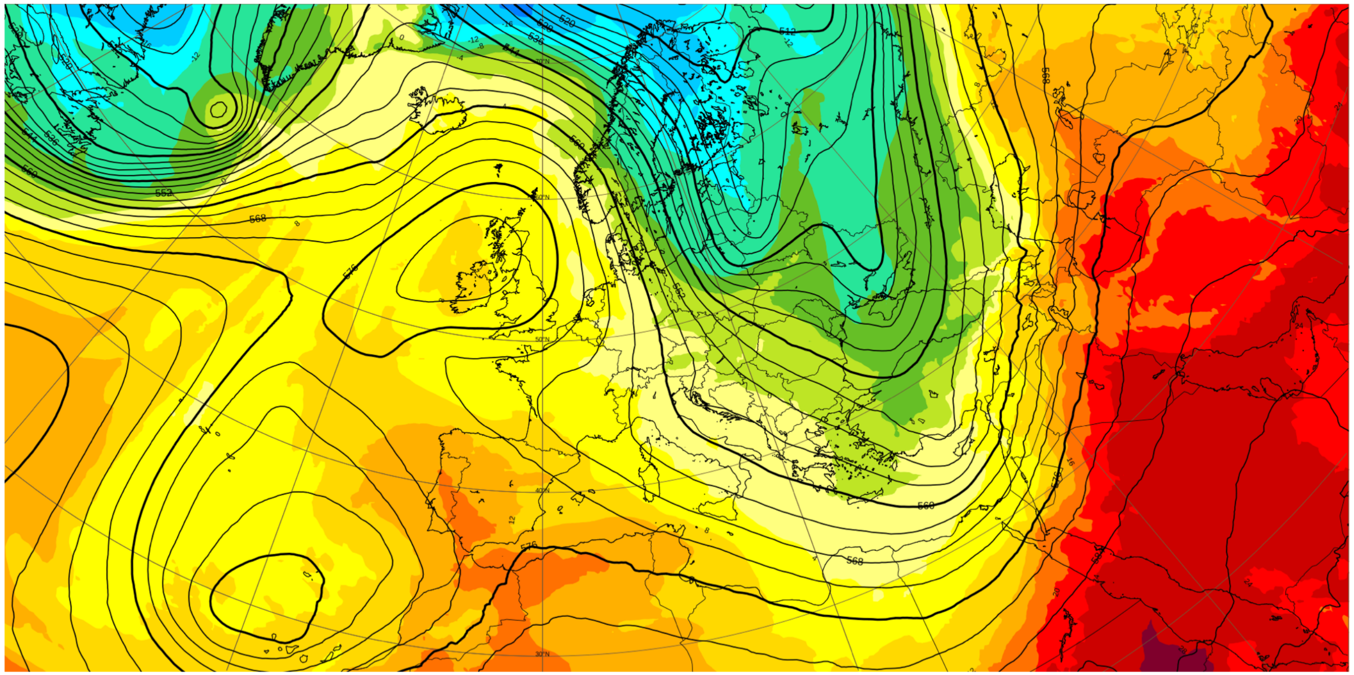

ECMWF

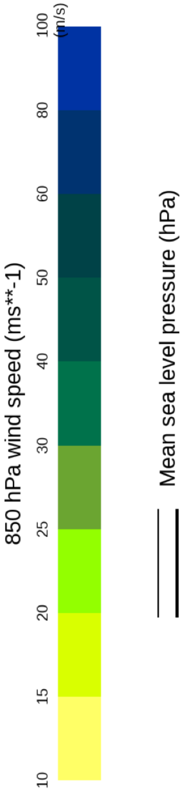

Base time: Fri 04 Apr 2025 12 UTC Valid time: Thu 10 Apr 2025 12 UTC (+144h) Area : Europe

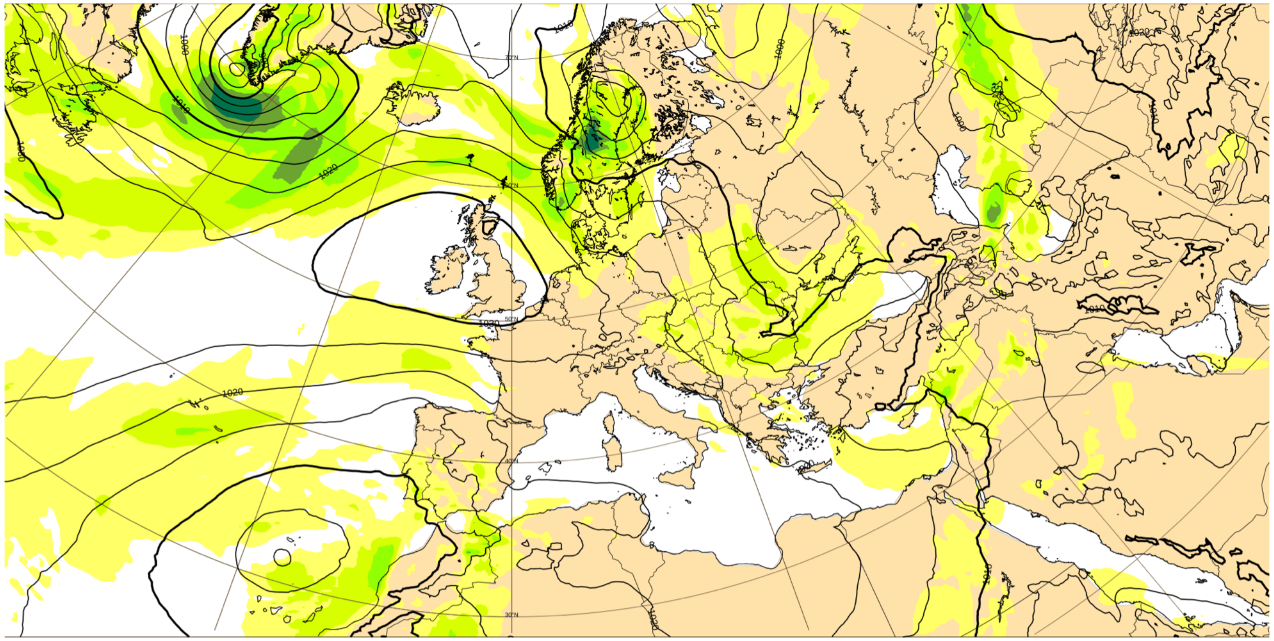

Base time: Thu 10 Apr 2025 00 UTC Valid time: Thu 10 Apr 2025 00 UTC (+0h) Area : Europe

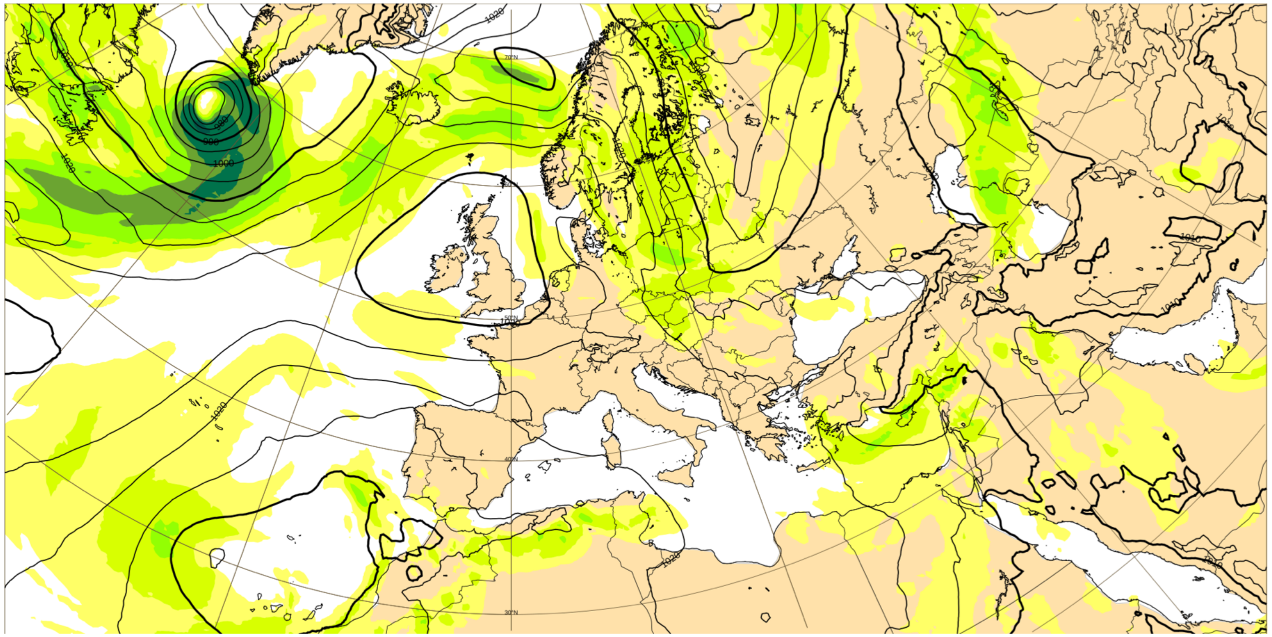

ECMWF

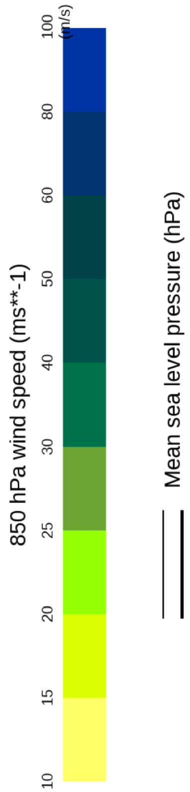

Base time: Fri 04 Apr 2025 12 UTC Valid time: Fri 04 Apr 2025 12 UTC (+0h) Area : Europe

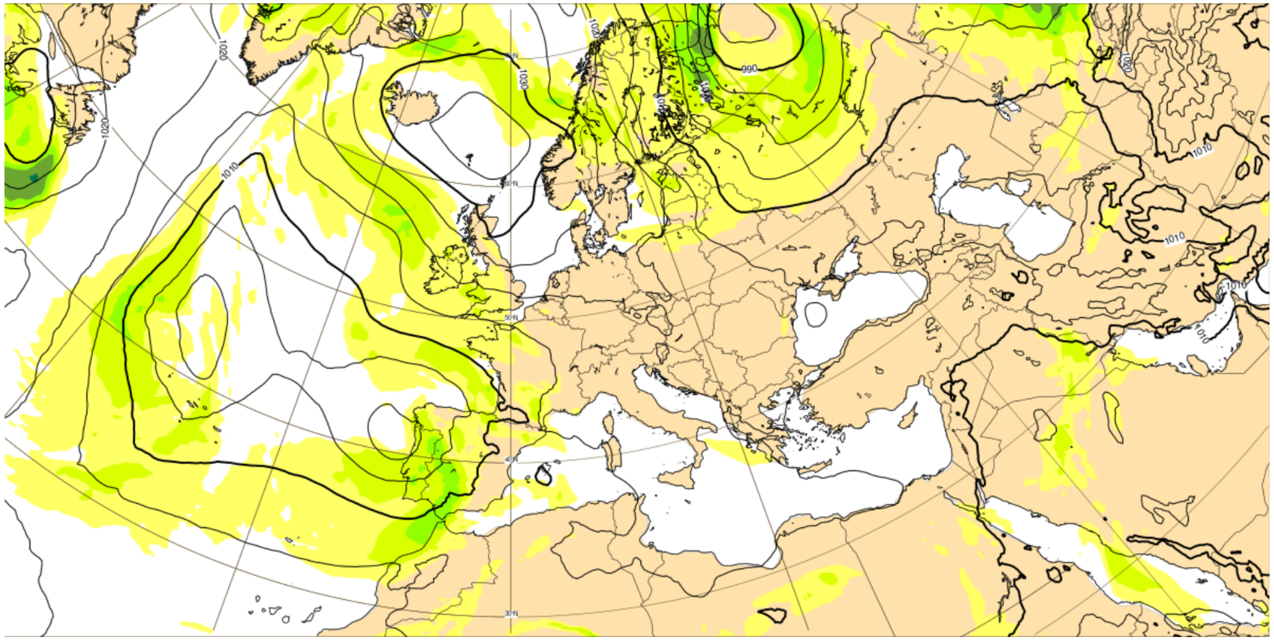

Base time: Thu 10 Apr 2025 00 UTC Valid time: Thu 10 Apr 2025 00 UTC (+0h) Area : Europe

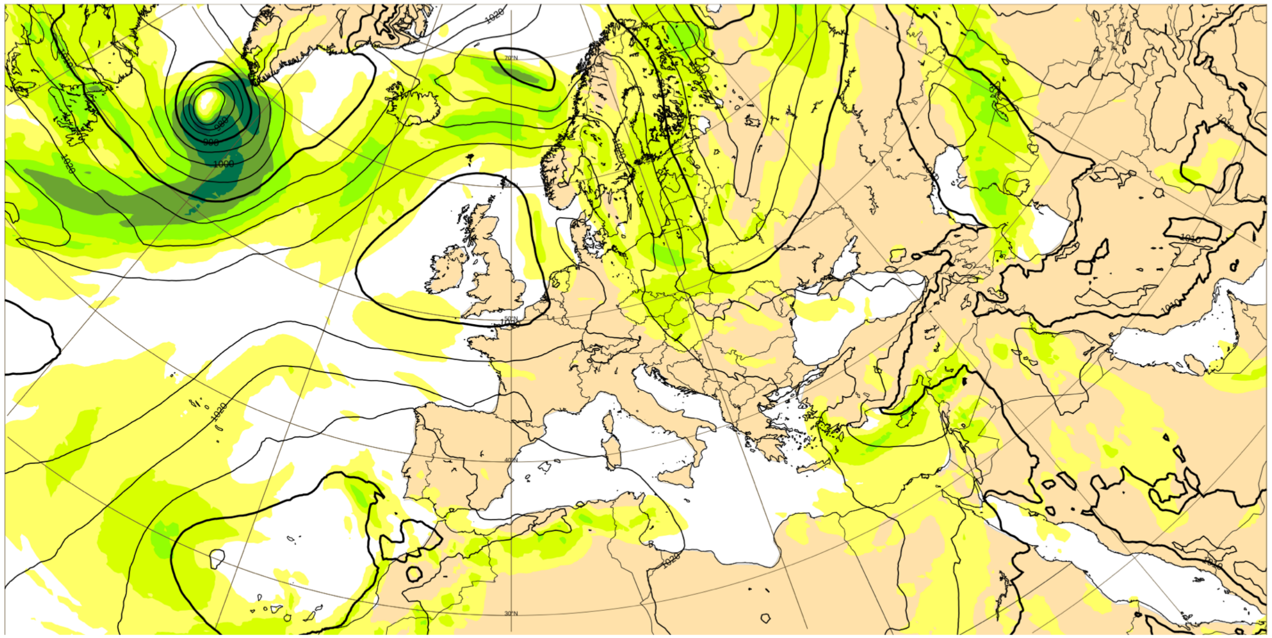

ECMWF

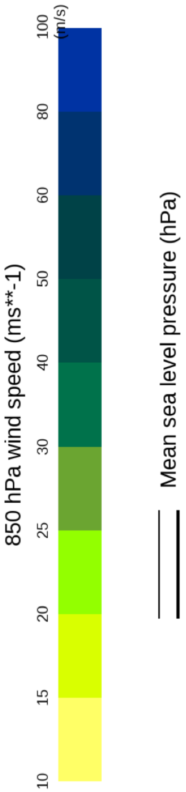

Base time: Wed 16 Mar 2022 00 UTC Valid time: Wed 23 Mar 2022 00 UTC (+168h) Area : Europe

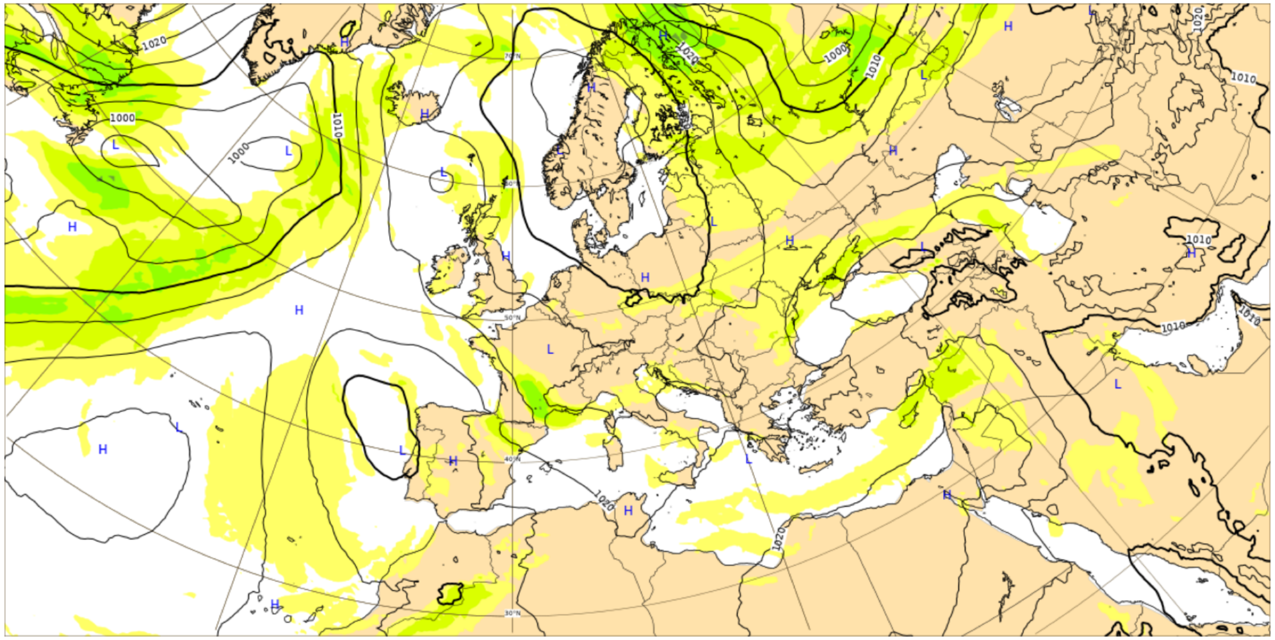

Base time: Wed 23 Mar 2022 00 UTC Valid time: Wed 23 Mar 2022 00 UTC (+0h) Area : Europe

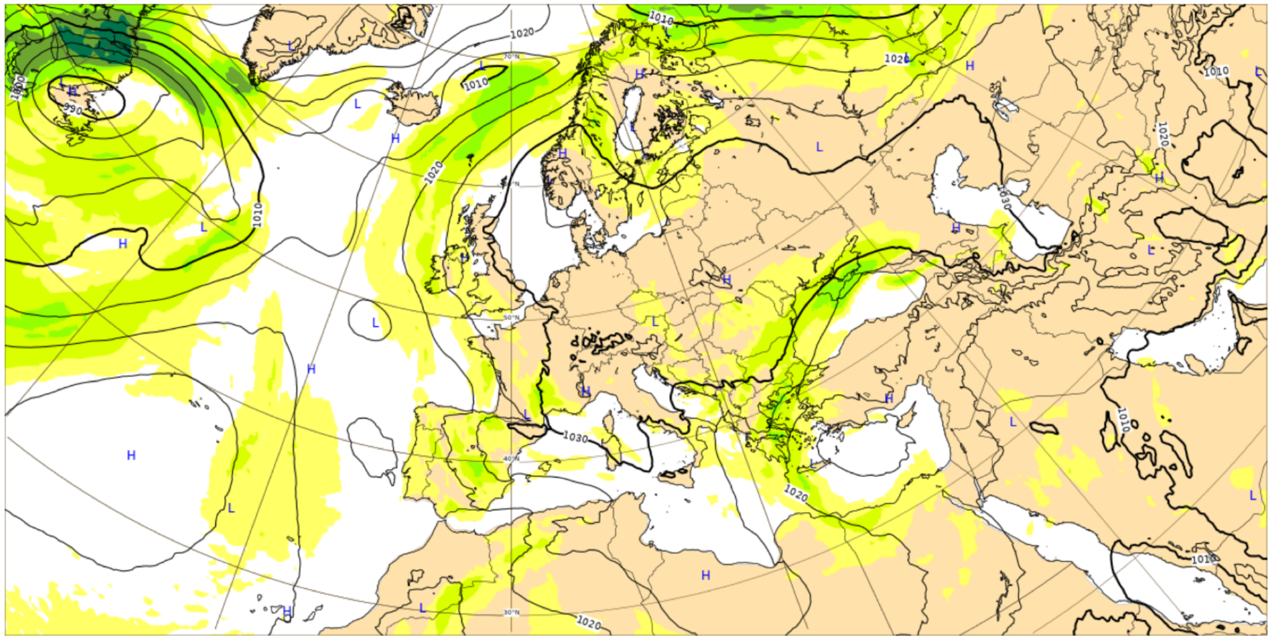

ECMWF

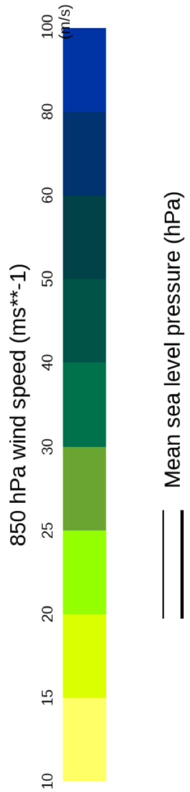

Base time: Wed 16 Mar 2022 00 UTC Valid time: Wed 16 Mar 2022 00 UTC (+0h) Area : Europe

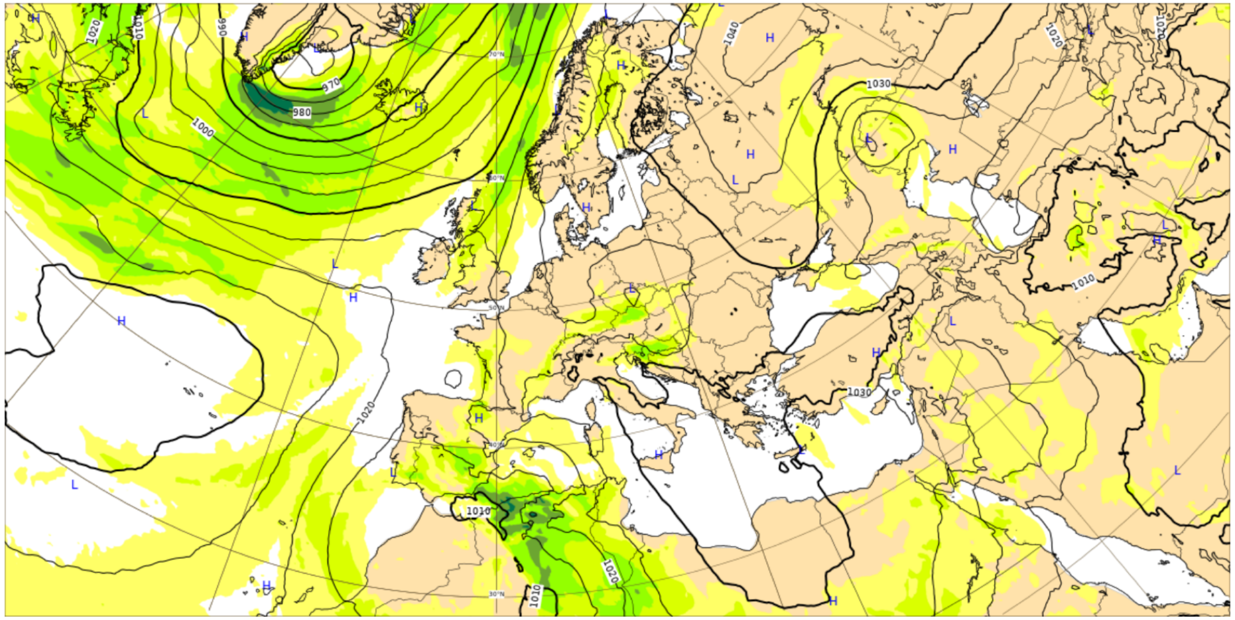

Base time: Wed 23 Mar 2022 00 UTC Valid time: Wed 23 Mar 2022 00 UTC (+0h) Area : Europe

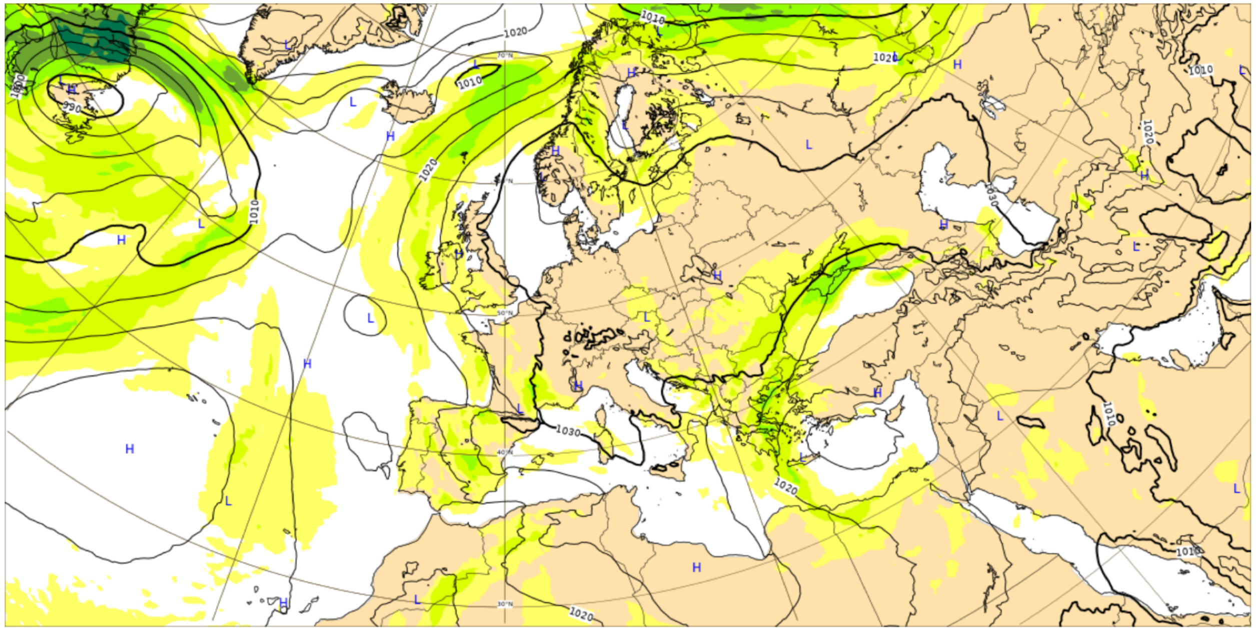

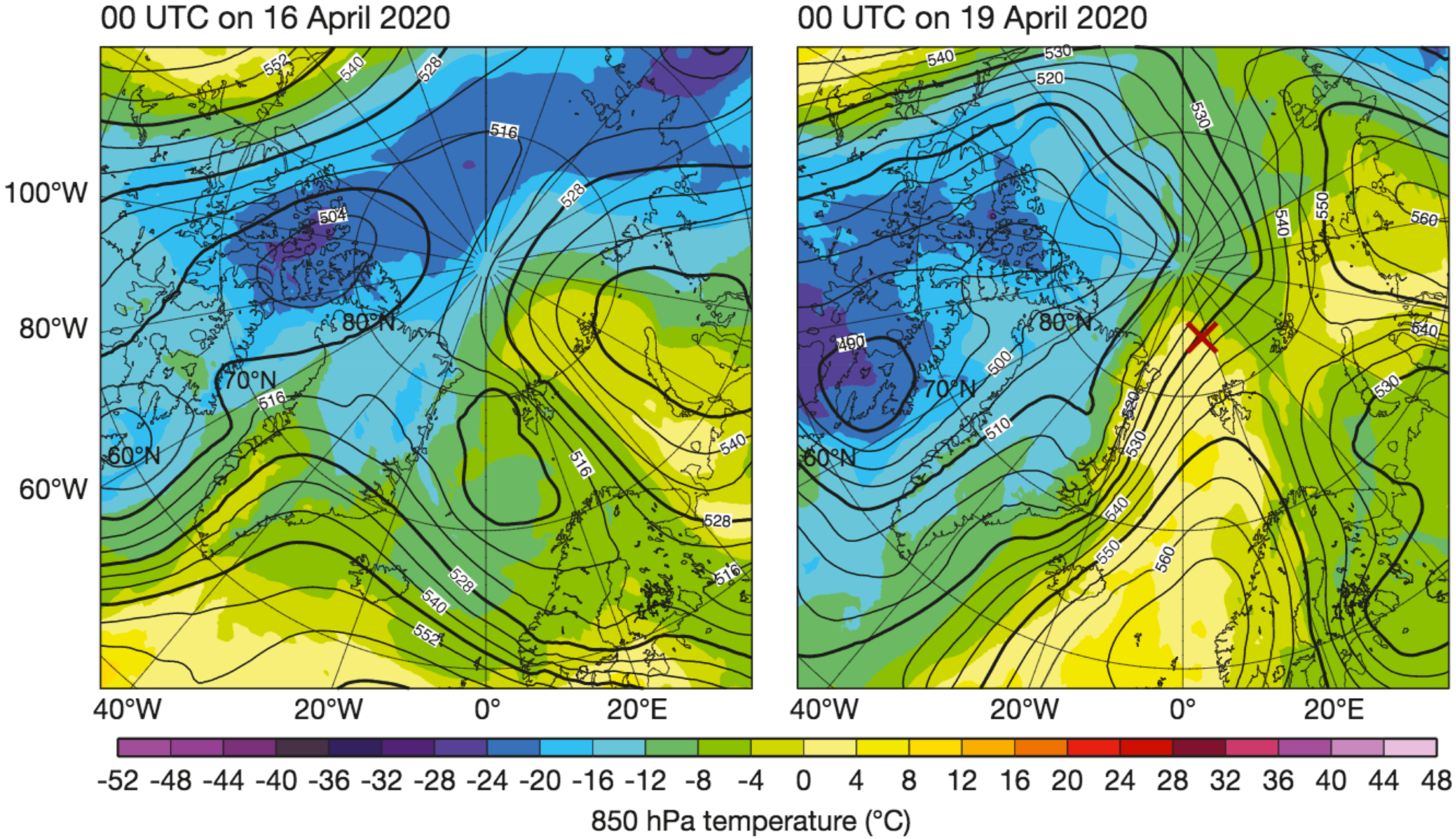

Synoptic situation on 16 and 19 April. Analysis of geopotential height at 500 hPa (contours) and temperature at 850 hPa (shading) for 00 UTC on 16 April 2020 (left) and 00 UTC on 19 April (right). The cross shows the approximate location of Polarstern on 19 April.

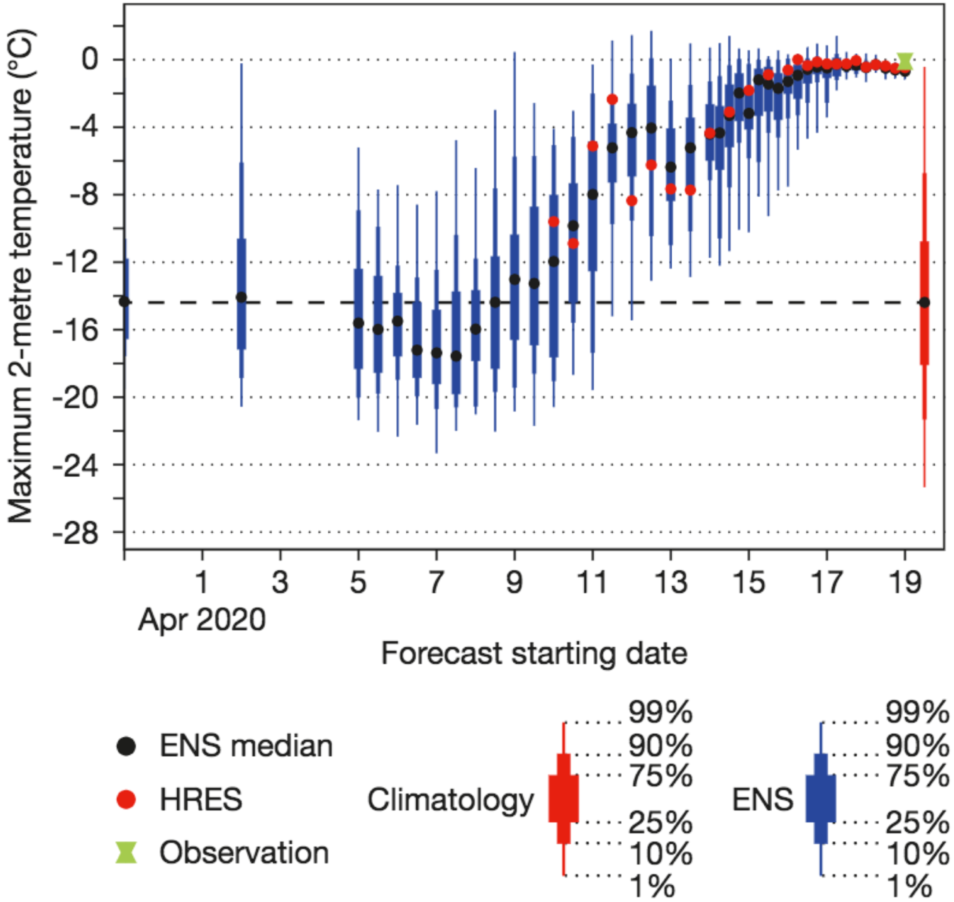

Evolution of forecasts for the 19 April warm air intrusion. The plot shows ensemble forecasts with different starting times for maximum 2-metre temperature for the Polarstern location on 19 April.

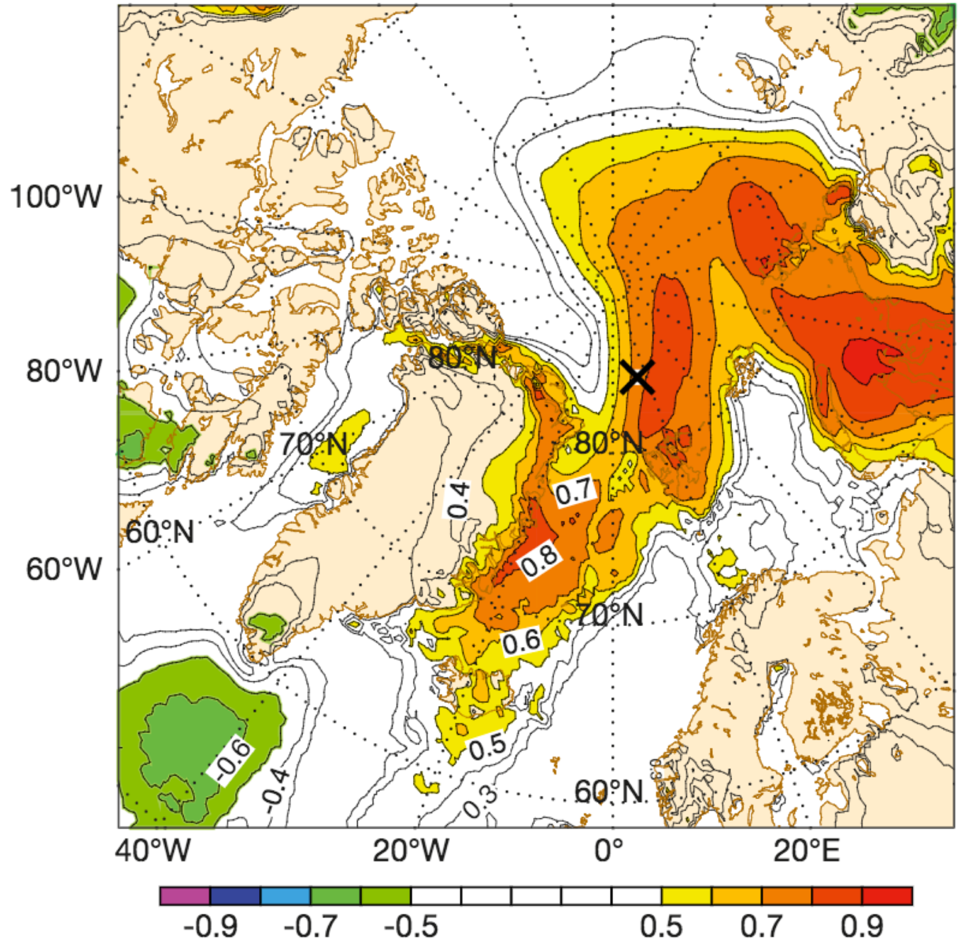

Two-metre maximum temperature EFI. The chart shows the 5-day forecast from 00 UTC on 15 April 2020 of the EFI for 2-metre maximum temperature on 19 April.

Results on site of ECMWF

In particular

- 09/2024. T. Haiden *et al., Evaluation of ECMWF forecasts,* Technical Memorandum 918, ECMWF, Reading, UK.

Available at the address :

1582-evaluation-of-ecmwf-forecasts.pdf

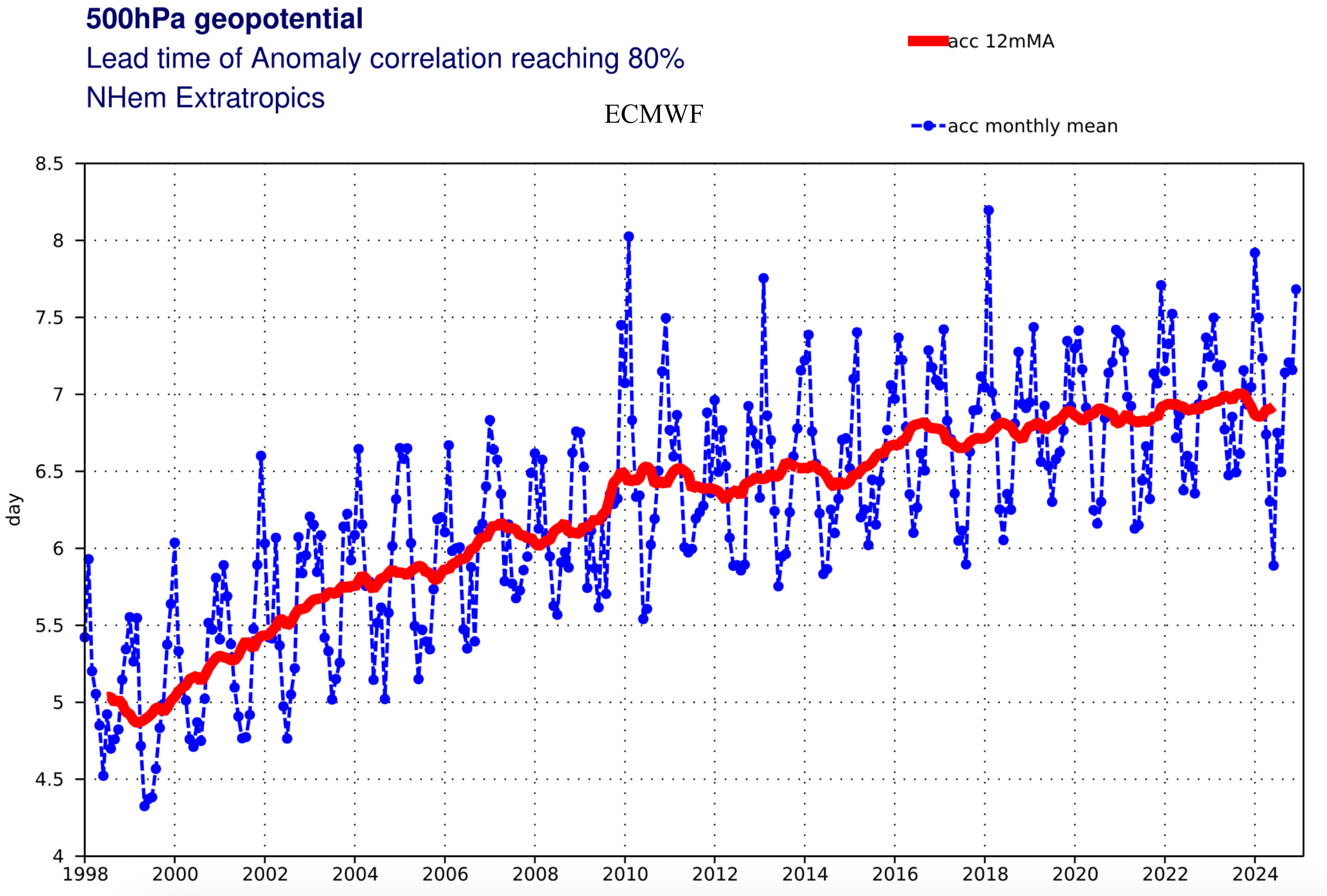

Spatial correlation between anomalies from climatology of forecast and verifying analysis

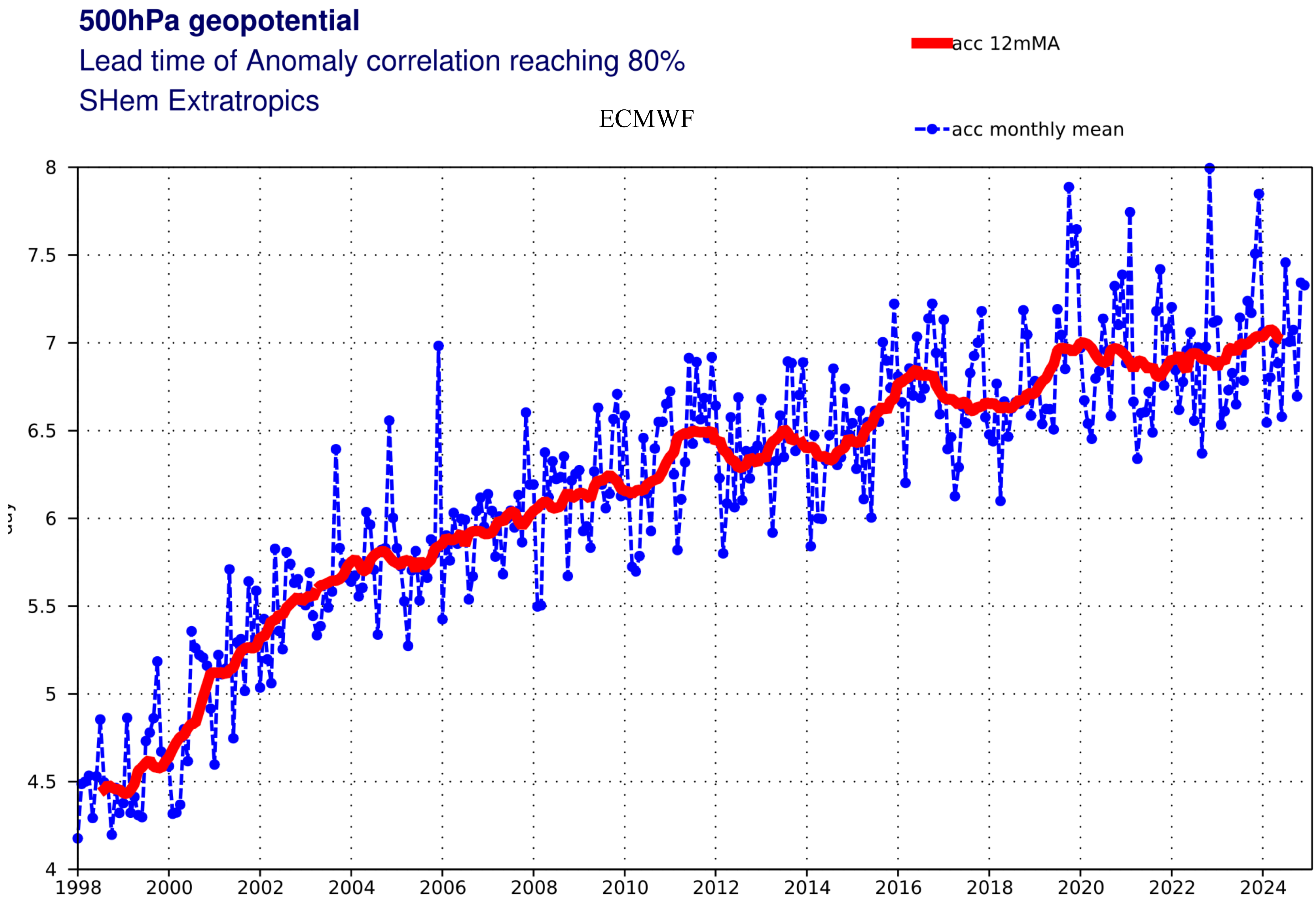

Spatial correlation between anomalies from climatology of forecast and verifying analysis

Lead time of anomaly correlation coefficient (ACC) reaching multiple thresholds (High resolution (HRES) 500 hPa height forecasts)

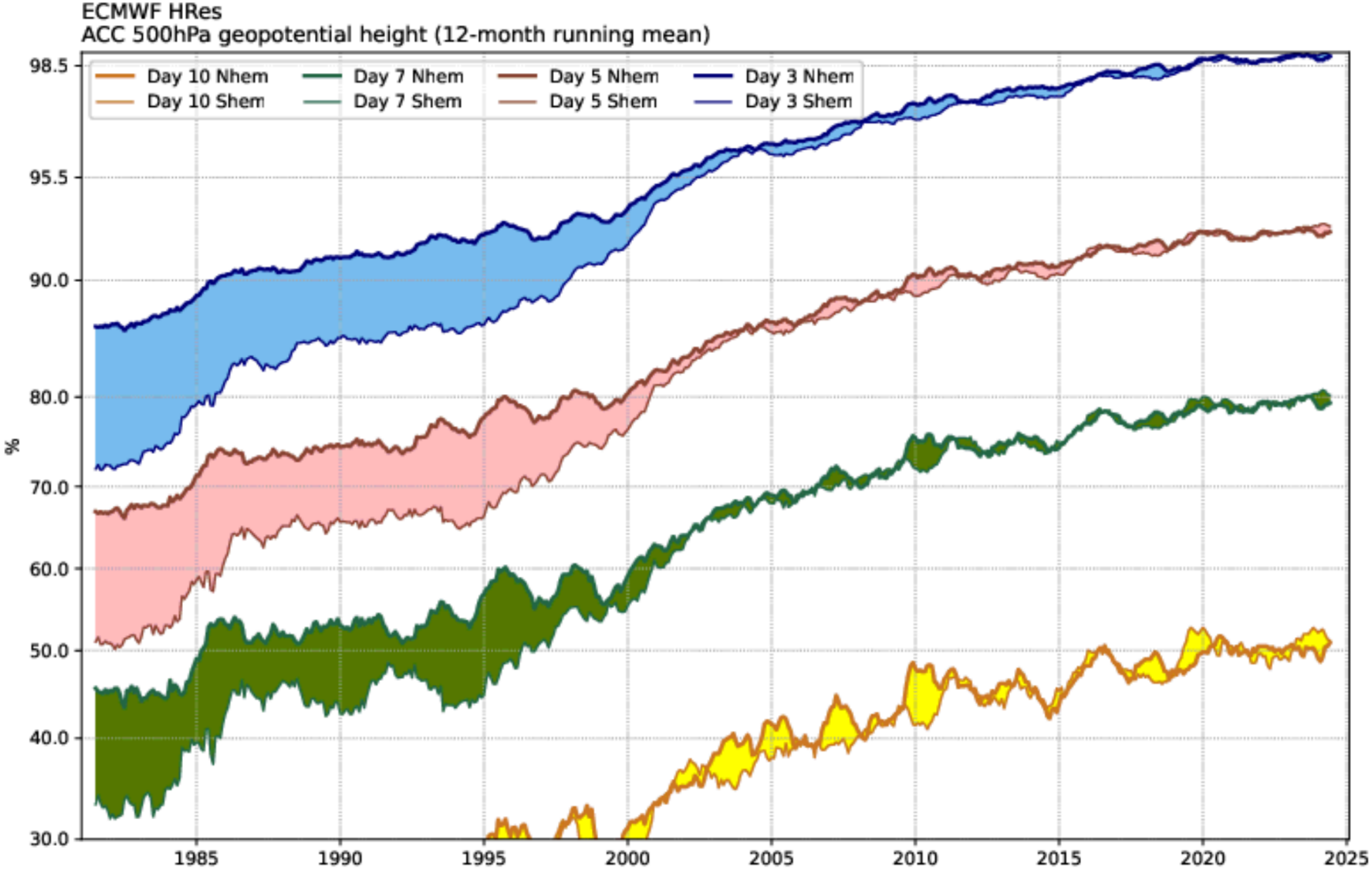

ECMWF

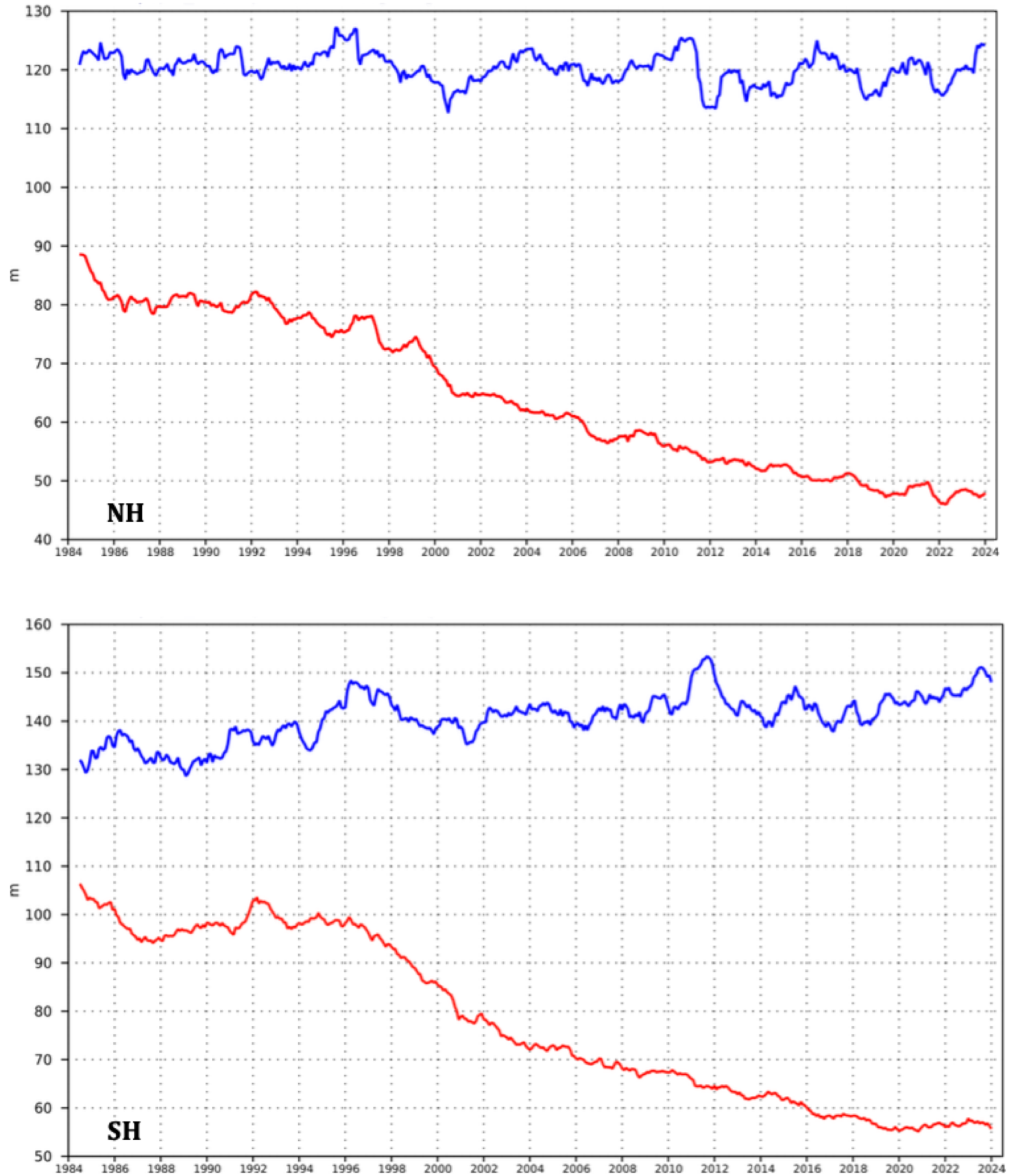

Figure 2: Root mean square (RMS) error of forecasts of 500 hPa geopotential height (m) at day 6 (red), verified against analysis. For comparison, a reference forecast made by persisting the analysis over 6 days is shown (blue). Plotted values are 12-month moving averages; the last point on the curves is for the 12-month period August 2023–July 2024. Results are shown for the northern extra-tropics (top), and the southern extra-tropics (bottom).

ECMWF

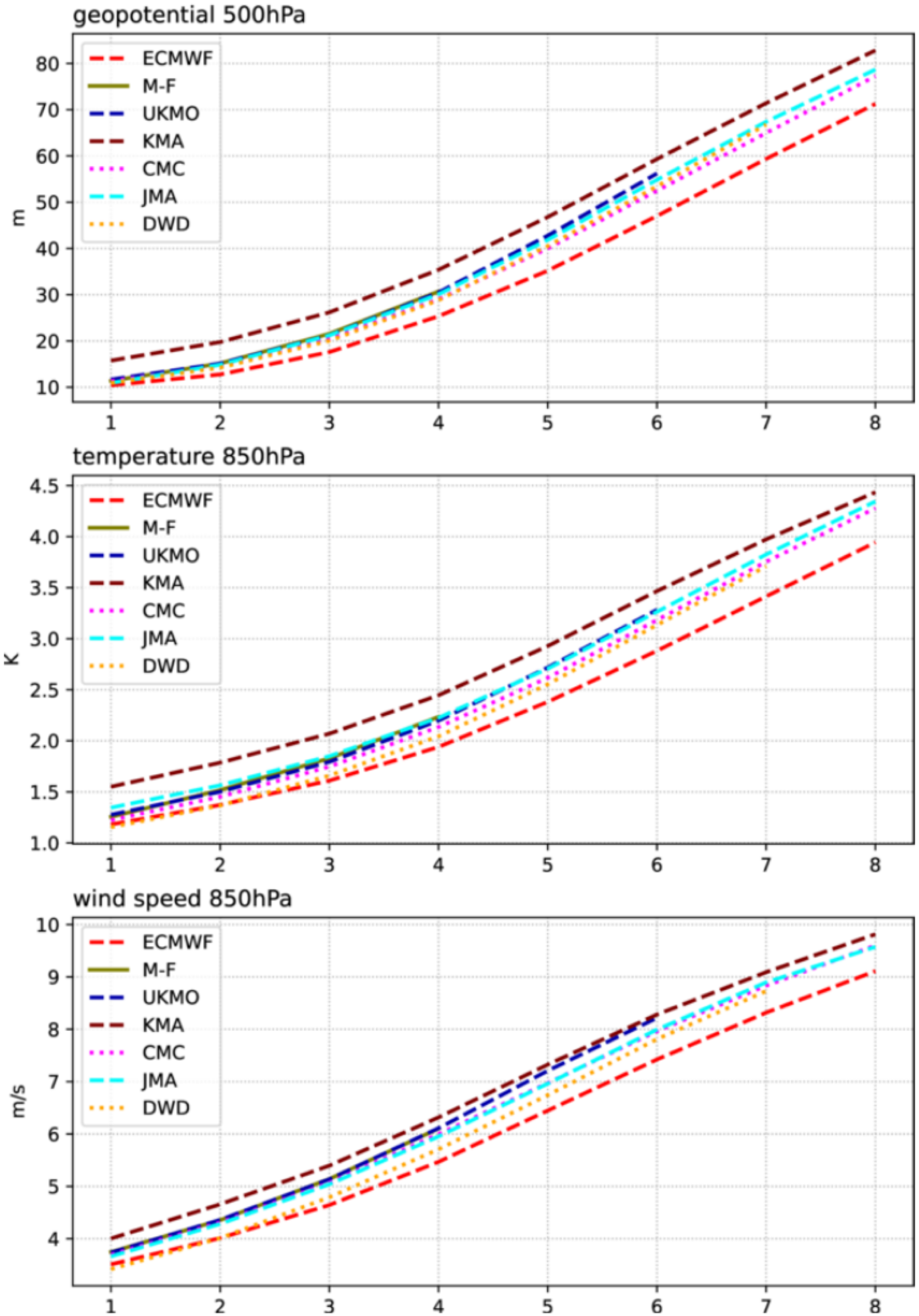

RMS forecast errors as functions of forecast range for different variables and forecasting centres (extratropical Northern Hemisphere)

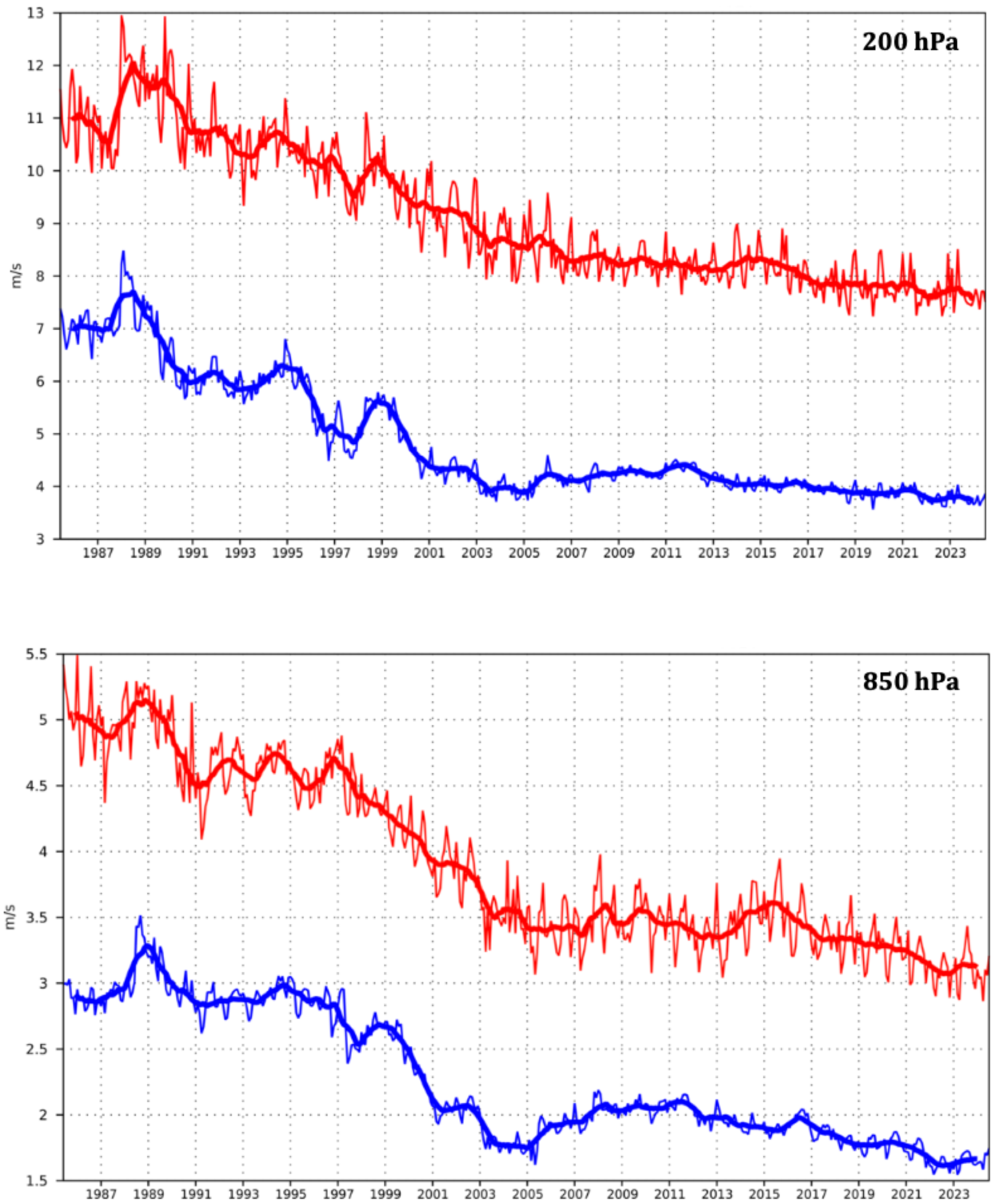

Figure 11: Forecast performance in the tropics. Curves show the monthly average RMS vector wind errors at 200 hPa (top) and 850 hPa (bottom) for one-day (blue) and five-day (red) forecasts, verified against analysis. 12-month moving average scores are also shown (in bold).

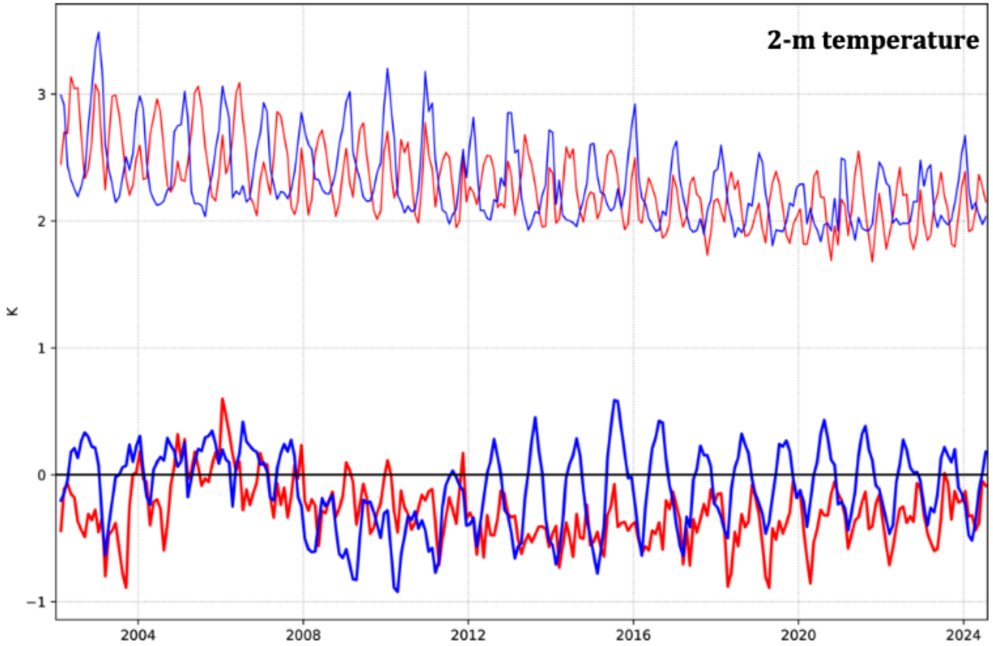

Figure 24: Verification of 2 m temperature forecasts against European SYNOP data on the GTS for 60-hour (night-time, blue) and 72-hour (daytime, red) forecasts. Lower pair of curves shows bias, upper curves are standard deviation of error.

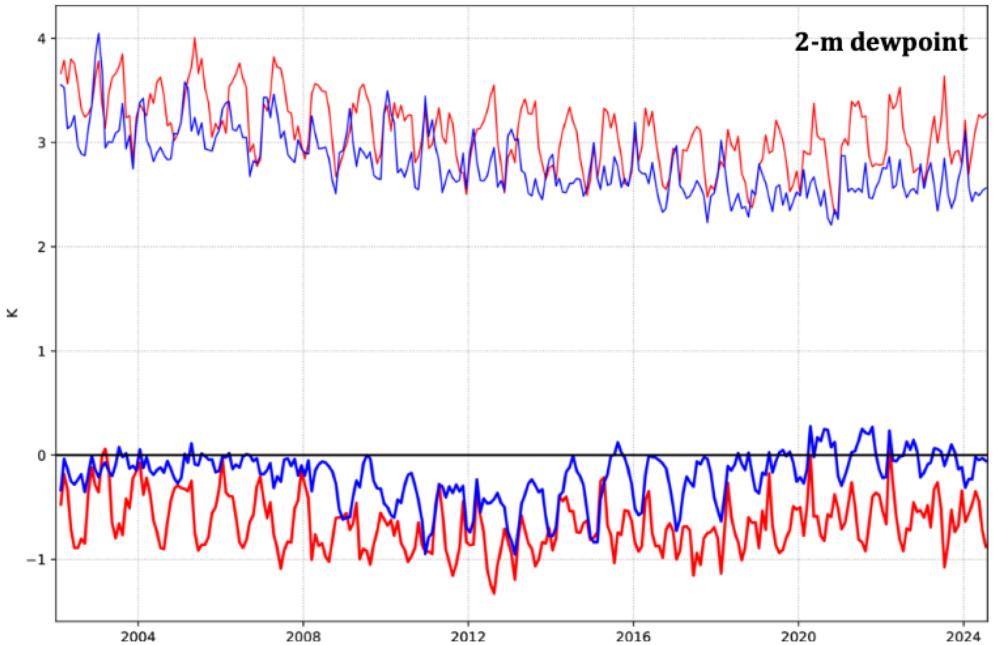

Figure 25: Verification of 2 m dew point forecasts against European SYNOP data on the Global Telecommunication System (GTS) for 60-hour (night-time, blue) and 72-hour (daytime, red) forecasts. Lower pair of curves shows bias, upper curves show standard deviation of error.

ECMWF

Europe

Night time: blue curves

Day time: red curves

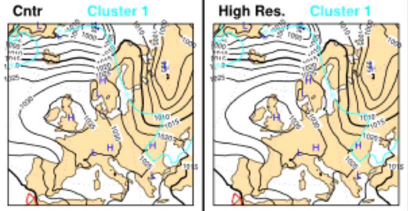

ECMWF ENSEMBLE FORECASTS

Thursday 03 April 2025 0000 UTC ECMWF forecast t+168 VT:Thursday 10 April 2025 0000 UTC
MSLP (contour every 5hPa) Temperature at 850hPa (only -6 and 16 isolines are plotted)

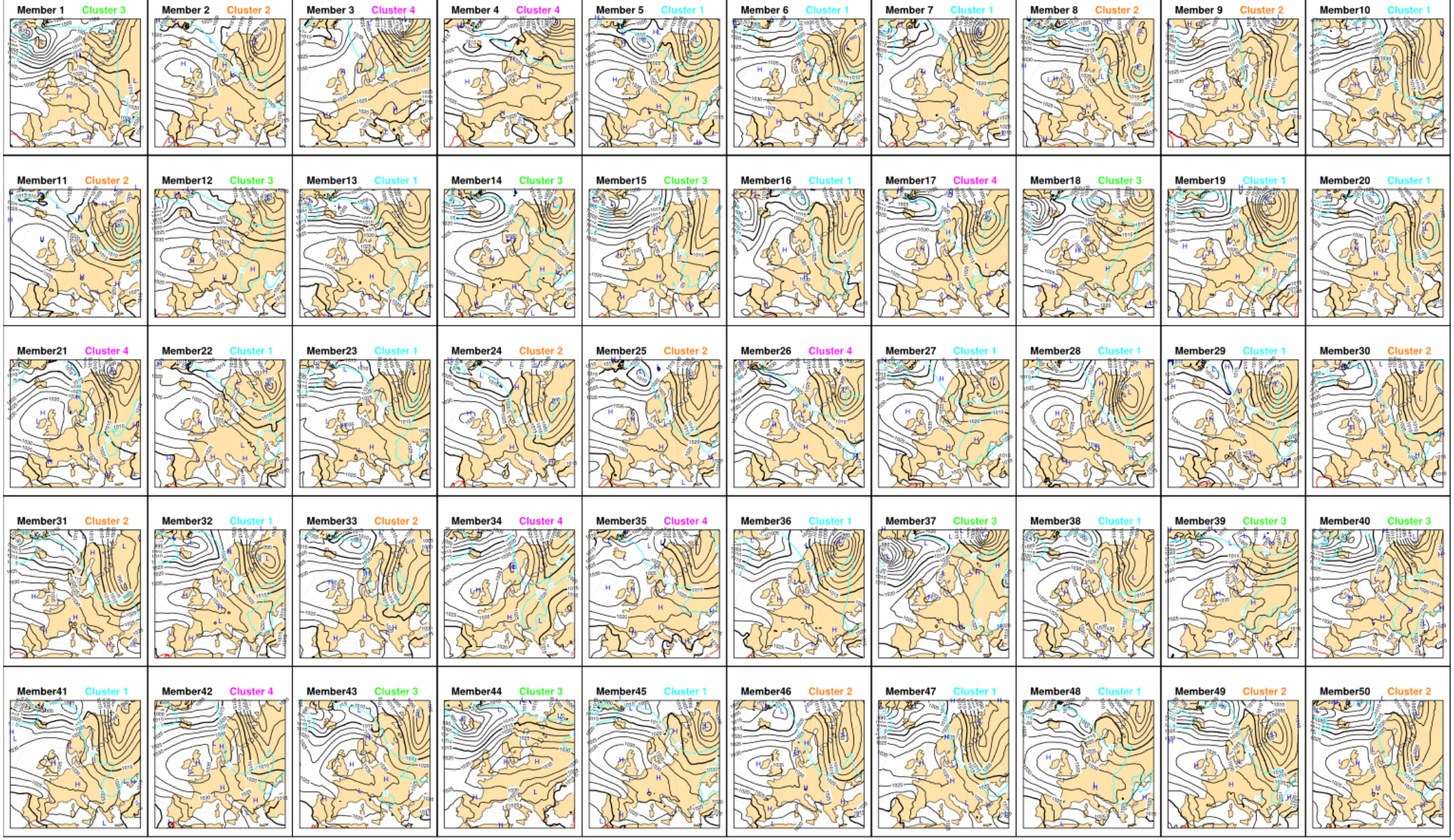

ECMWF

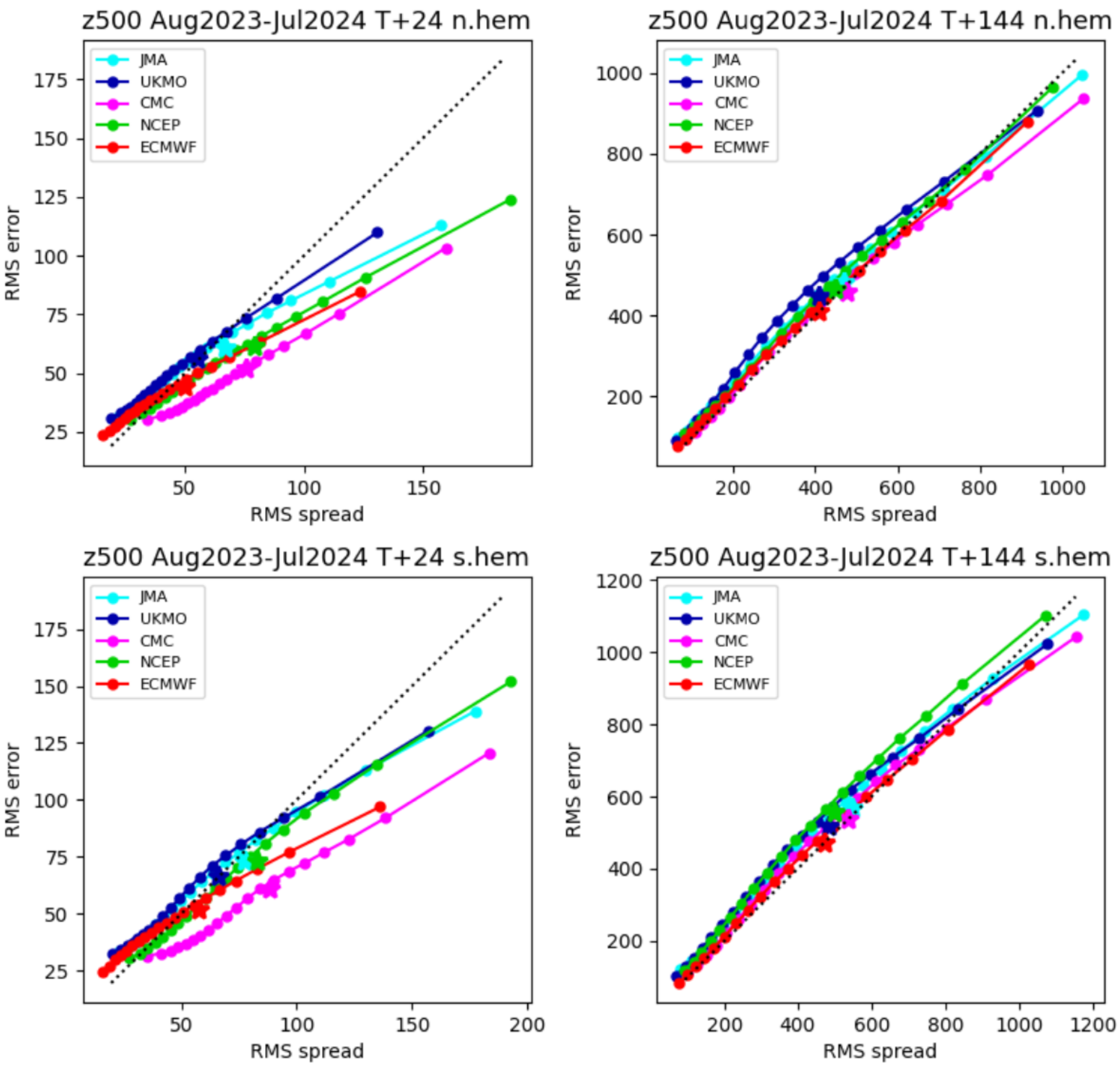

Figure 8: Ensemble spread reliability of different global models for 500 hPa geopotential for the period August 2023–July 2024 in the northern (top) and southern (bottom) hemisphere extra-tropics for day 1 (left) and day 6 (right), verified against analysis. Circles show error for different values of spread, stars show average error-spread relationship.

ECMWF

Continuous Ranked Probability Skill Score measures both reliability and resolution

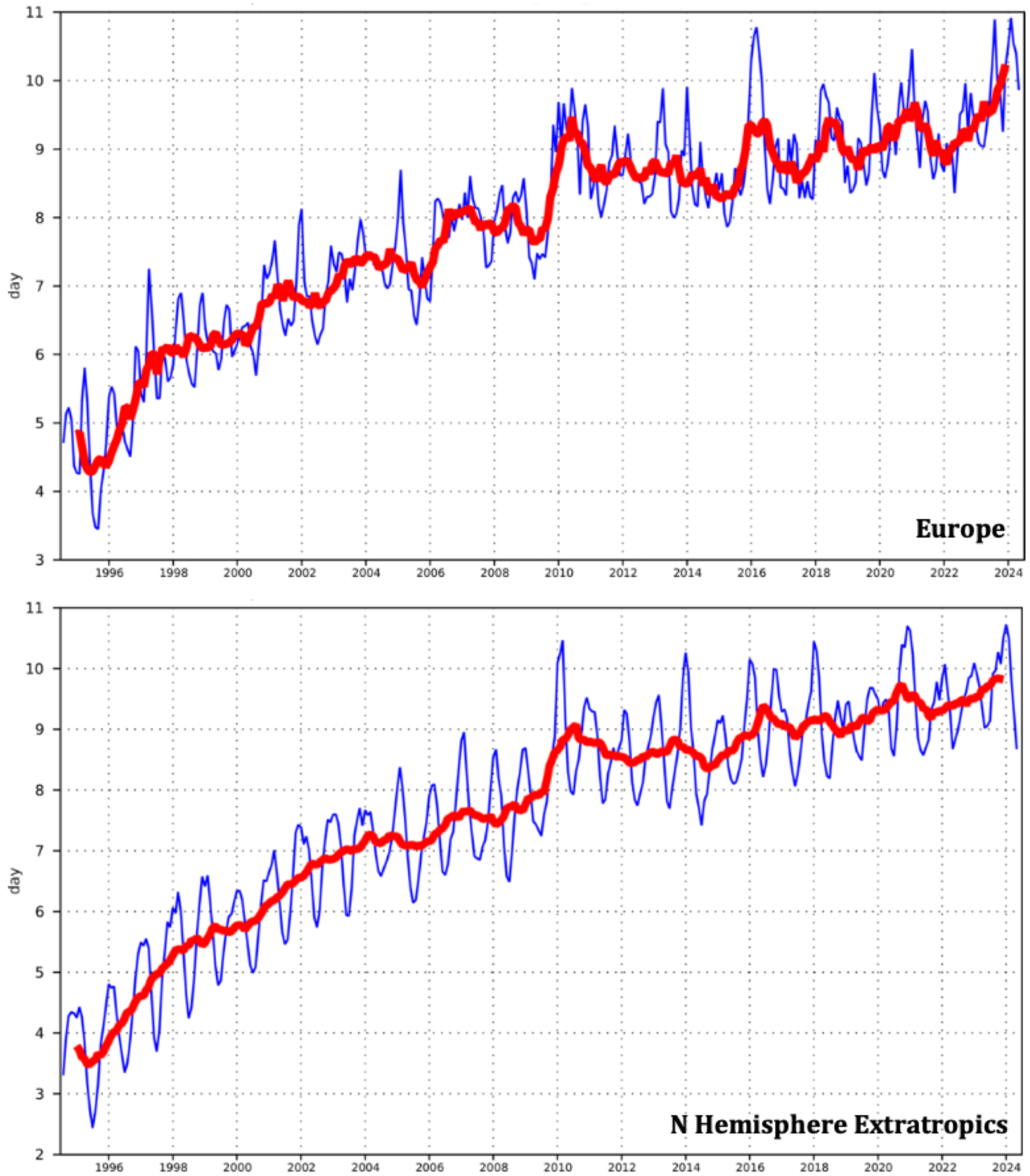

Figure 6: Primary headline score for the ensemble probabilistic forecasts. Evolution with time of 850 hPa temperature ensemble forecast performance, verified against analysis. Each point on the curves is the forecast range at which the 3-month mean (blue lines) or 12-month mean centred on that month (red line) of the continuous ranked probability skill score (CPRSS) falls below 25% for Europe (top), northern hemisphere extratropics (bottom).

Remaining problems

- Water cycle (evaporation, condensation, influence on absorbed or emitted radiation)

- Exchanges with ocean or continental surface (heat, water, momentum, …)

- …

That is for physical approach to prediction, based on known physical laws

Another approach is now being developed, based on ***Machine Learning*** (aka ***Deep Learning***)

Why not directly use observations (for instance, in the case of a weather forecast, why not look for analogues in the past, and make the forecast from those analogues) ?

E. N. Lorenz (1960s). Sample of past observations will never be large enough for competing with physically-based models.

But :

- there is no incompatibility between the two approaches

- there remain many processes in numerical models which we do not know how to describe on the basis of well-established physical laws (interactions between atmosphere and underlying medium, such as *e.g.* vegetation, all kinds of subgrid scale processes, …)

- amount of data of all kinds, as well as computing power, are increasing very rapidly.

Machine Learning (continuation)

Powerful numerical tools have been developed for the exploitation of very large sets of data (*big data*)

Neural networks. Define an explicit numerical link between an *input set* and an *output set.* Define function F such that, to some useful degree of approximation

$$\boldsymbol{y} = \boldsymbol{F}(\boldsymbol{x})$$

where x and y belong to the input and output sets respectively.

The function $\boldsymbol{F}$ is typically built as a composition of *sigmoid functions*

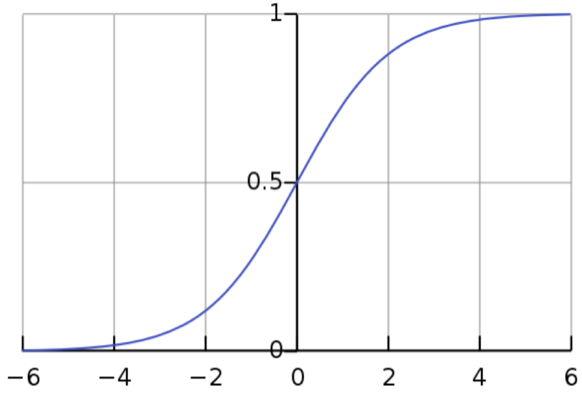

Machine Learning (continuation 2)

Neural networks have turned out to be extremely efficient in many applications. In the context of assimilation of observations, they have been used for defining for instance the observation operators (***H***) corresponding to satellite observations. But they have been used more recently, in evaluation studies and on idealized situations, but with some success, for determining 'dynamical laws'.

Machine Learning (continuation 3)

And, more importantly, they have been used for developing softwares for meteorological predictions at a range of a few days, using as training ensembles reanalyses produced by meteorological centres.

ECMWF has for instance developed the *AIFS* software, with its own ERA5 reanalysis (1979-present) as training ensemble. The forecasts thus obtained are of similar quality as those of HRES, but at a much lower numerical cost (a few minutes, instead of a few hours, for a 10-day forecast).

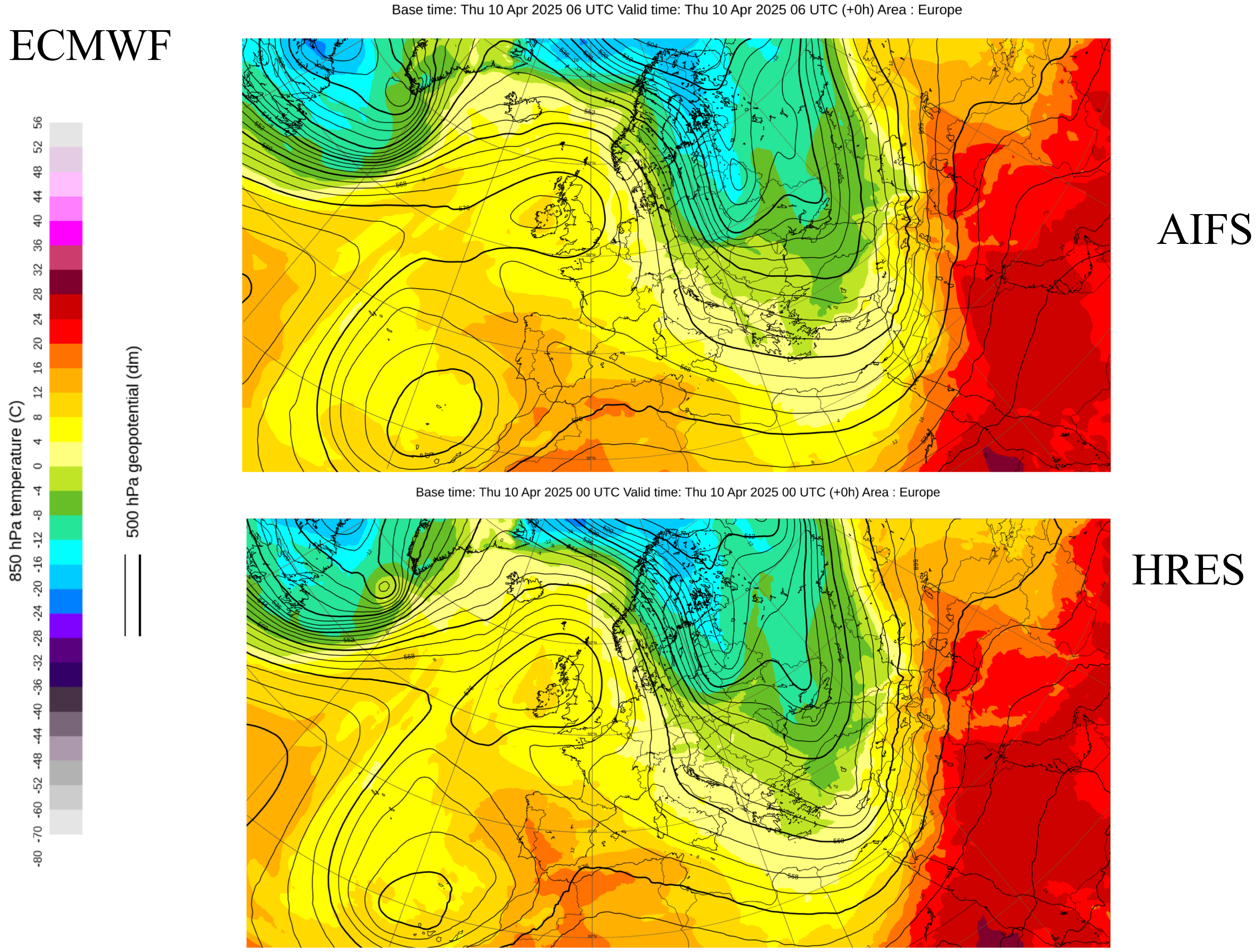
ECMWF
Base time: Thu 10 Apr 2025 06 UTC Valid time: Thu 10 Apr 2025 06 UTC (+0h) Area : Europe
AIFS
Base time: Thu 10 Apr 2025 00 UTC Valid time: Thu 10 Apr 2025 00 UTC (+0h) Area : Europe
HRES
850 hPa temperature (C)
500 hPa geopotential (dm)
-80 -70 -60 -52 -48 -44 -40 -36 -32 -28 -24 -20 -16 -12 -8 -4 0 4 8 12 16 20 24 28 32 36 40 44 48 52 56

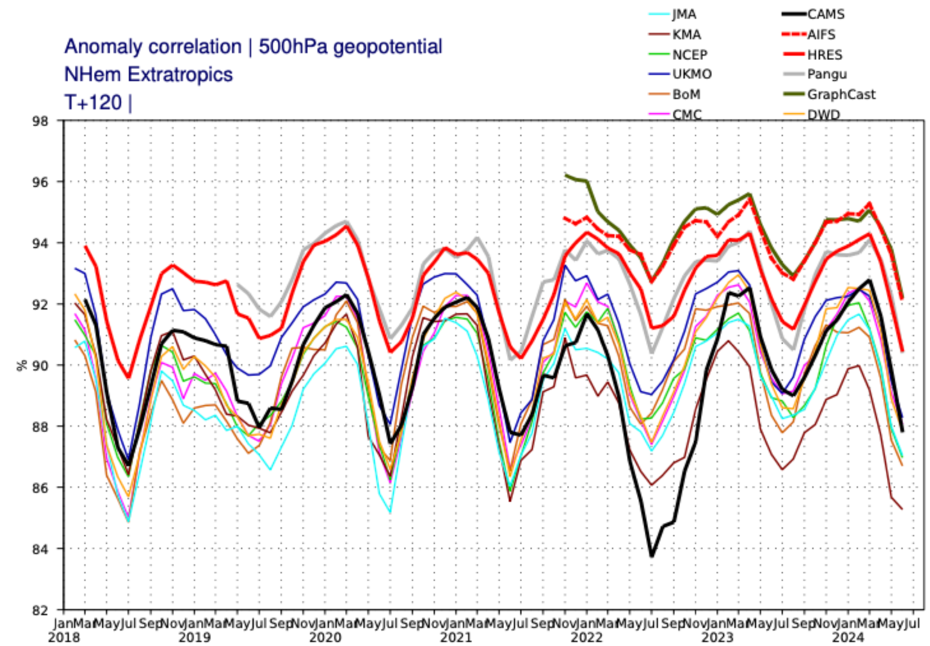

Figure 17: Anomaly correlation of 500 hPa geopotential in the northern hemisphere extratropics at day 5. CAMS forecast (black) shown in comparison to the HRES (red) and forecasts from other global centres (thin lines). Also shown are forecasts from machine learning (ML) models: GraphCast (olive), Pangu (grey), and AIFS (red dashes).

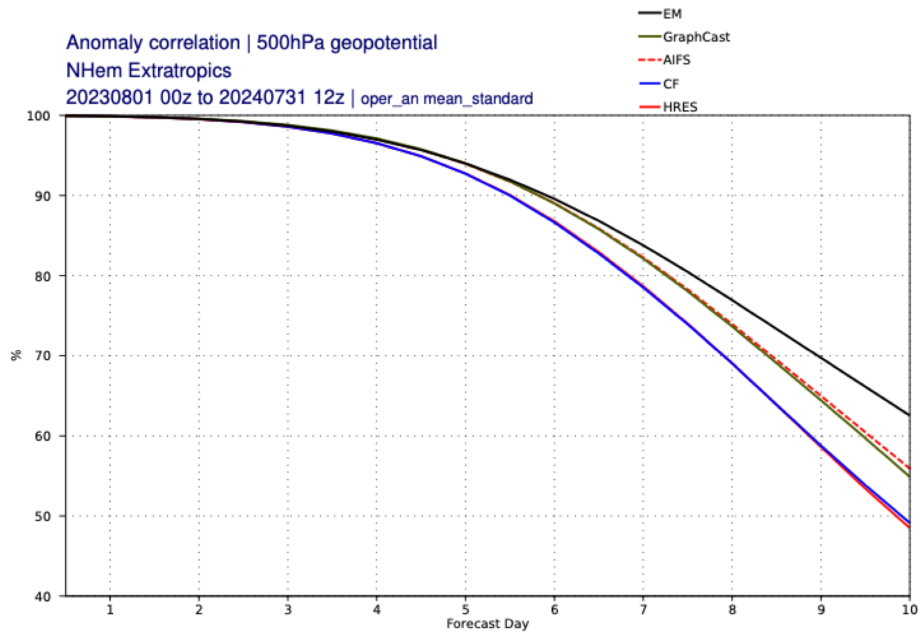

Figure 18: Anomaly correlation of 500 hPa geopotential in the northern extratropics for the 12-month period Aug 2023 to July 2024. Black: ENS mean, olive: GraphCast ML forecast, red dashes: AIFS, blue: ENS control, red: HRES.

ECMWF data coverage (all observations) - SYNOP-SHIP-METAR
2025040921 to 2025041003
Total number of obs = 242165

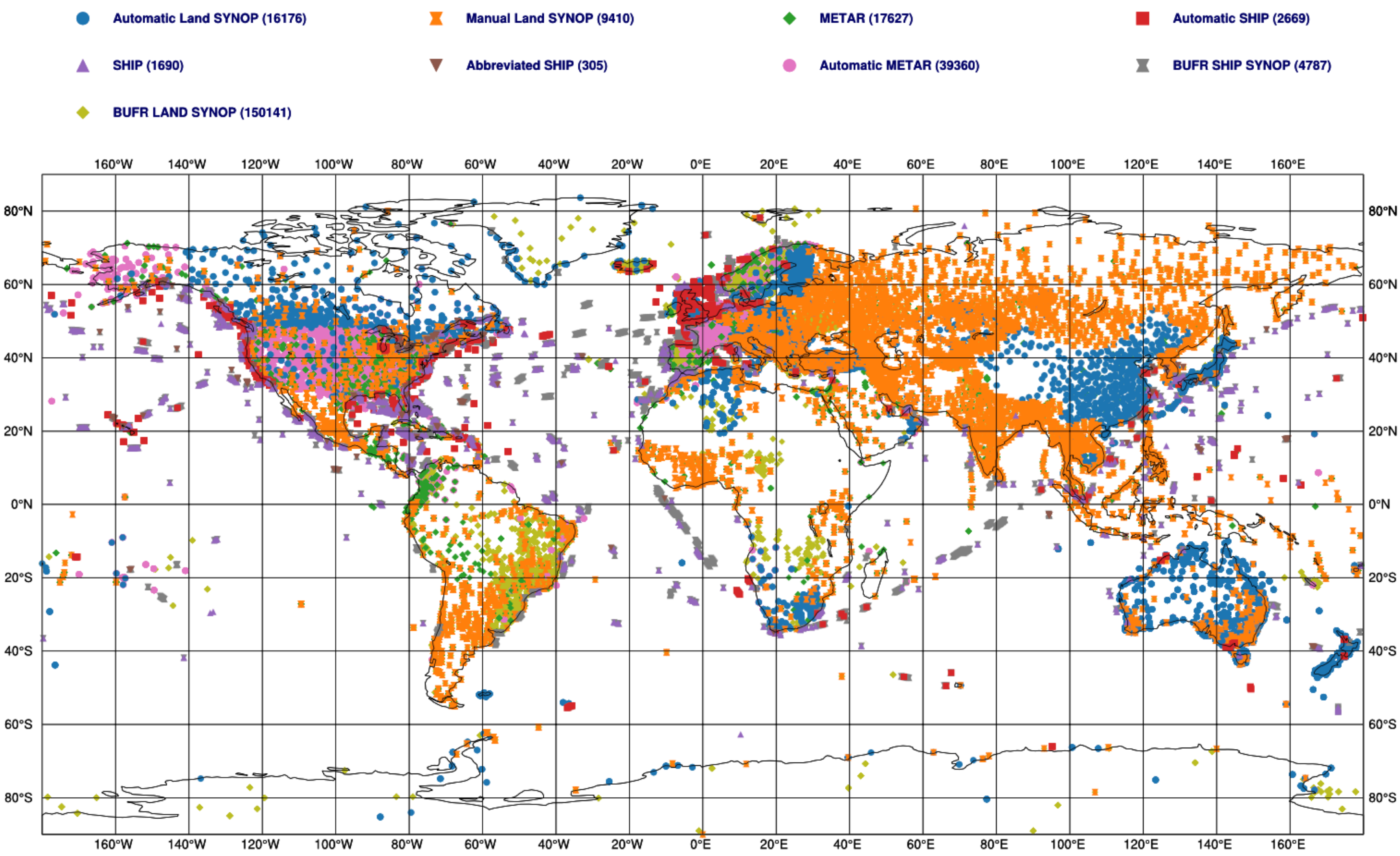

ECMWF data coverage (all observations) - RADIOSONDE
2025040921 to 2025041003
Total number of obs = 1093

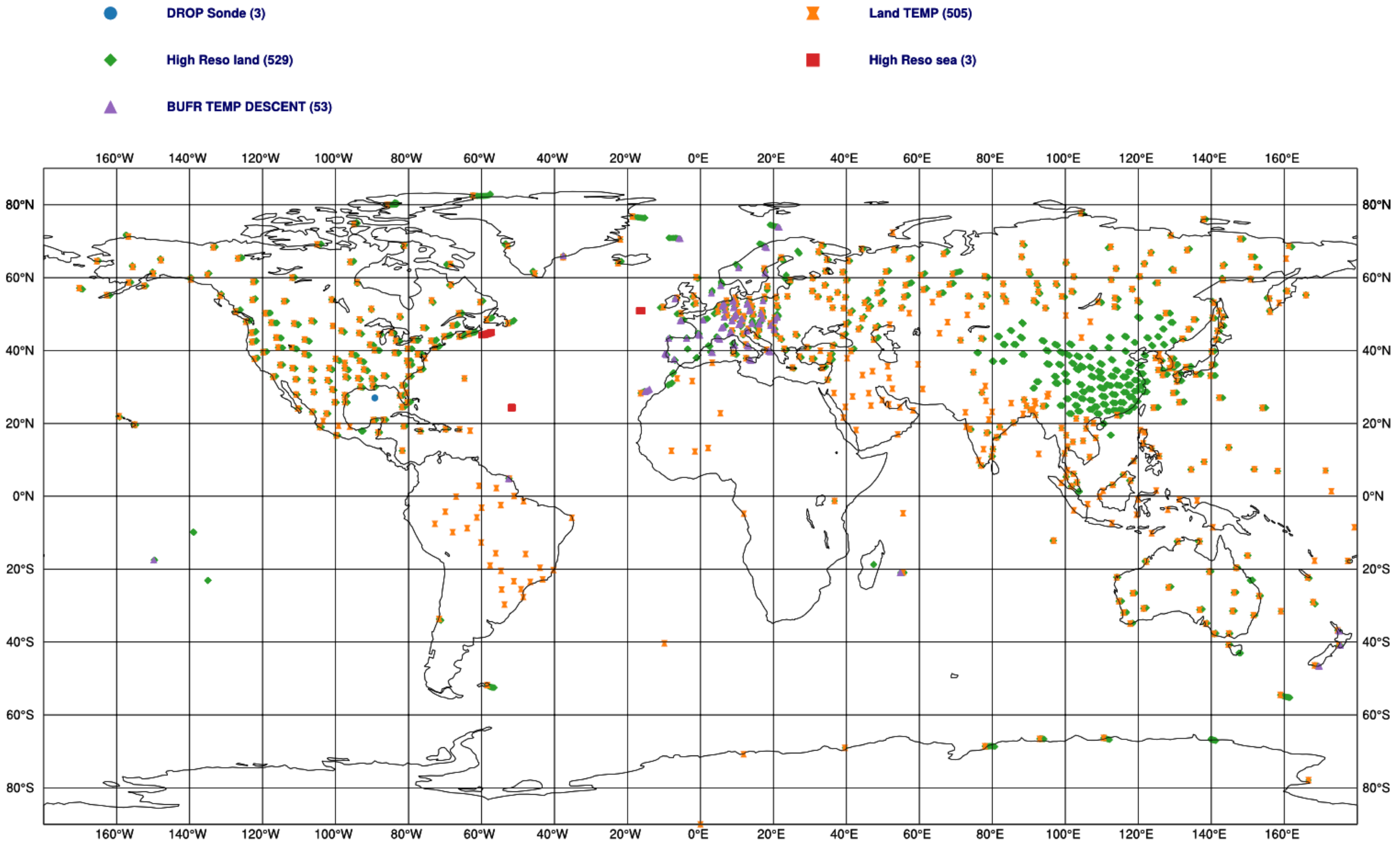

ECMWF data coverage (all observations) - AIRCRAFT
2025040921 to 2025041003
Total number of obs = 741617

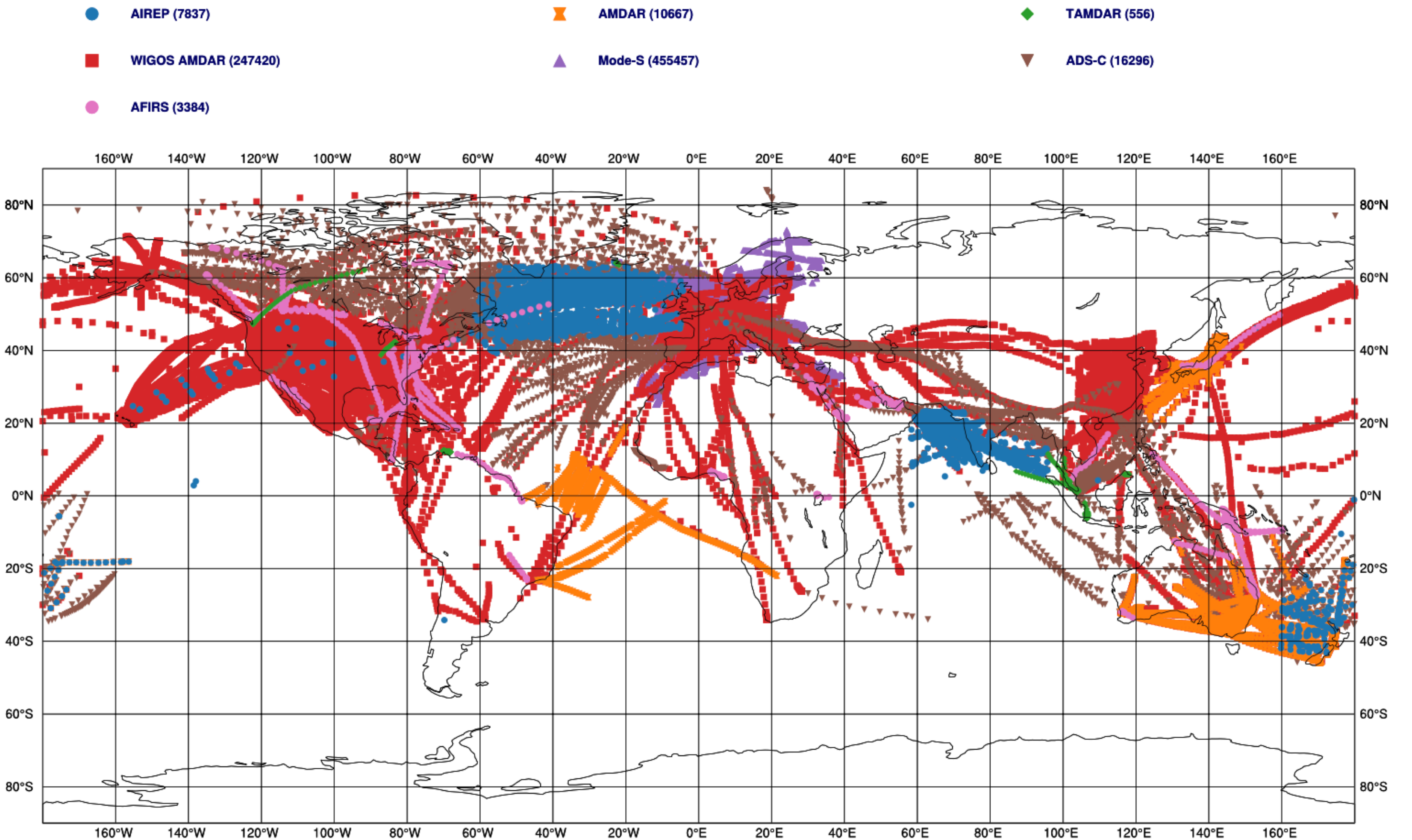

ECMWF data coverage (all observations) - AMSUA
2025040921 to 2025041003
Total number of obs = 93786

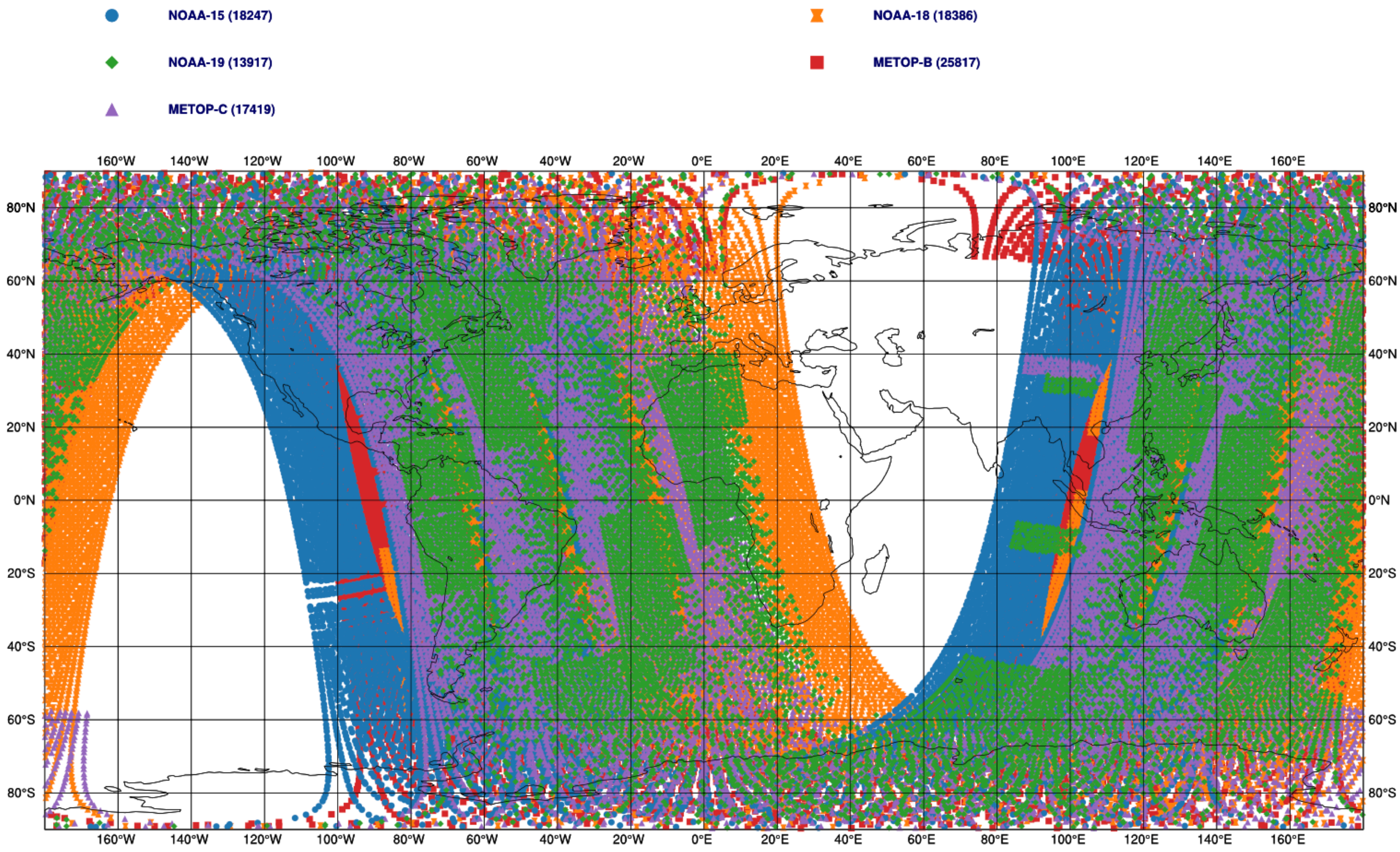

ECMWF data coverage (all observations) - IASI
2025040921 to 2025041003
Total number of obs = 167863

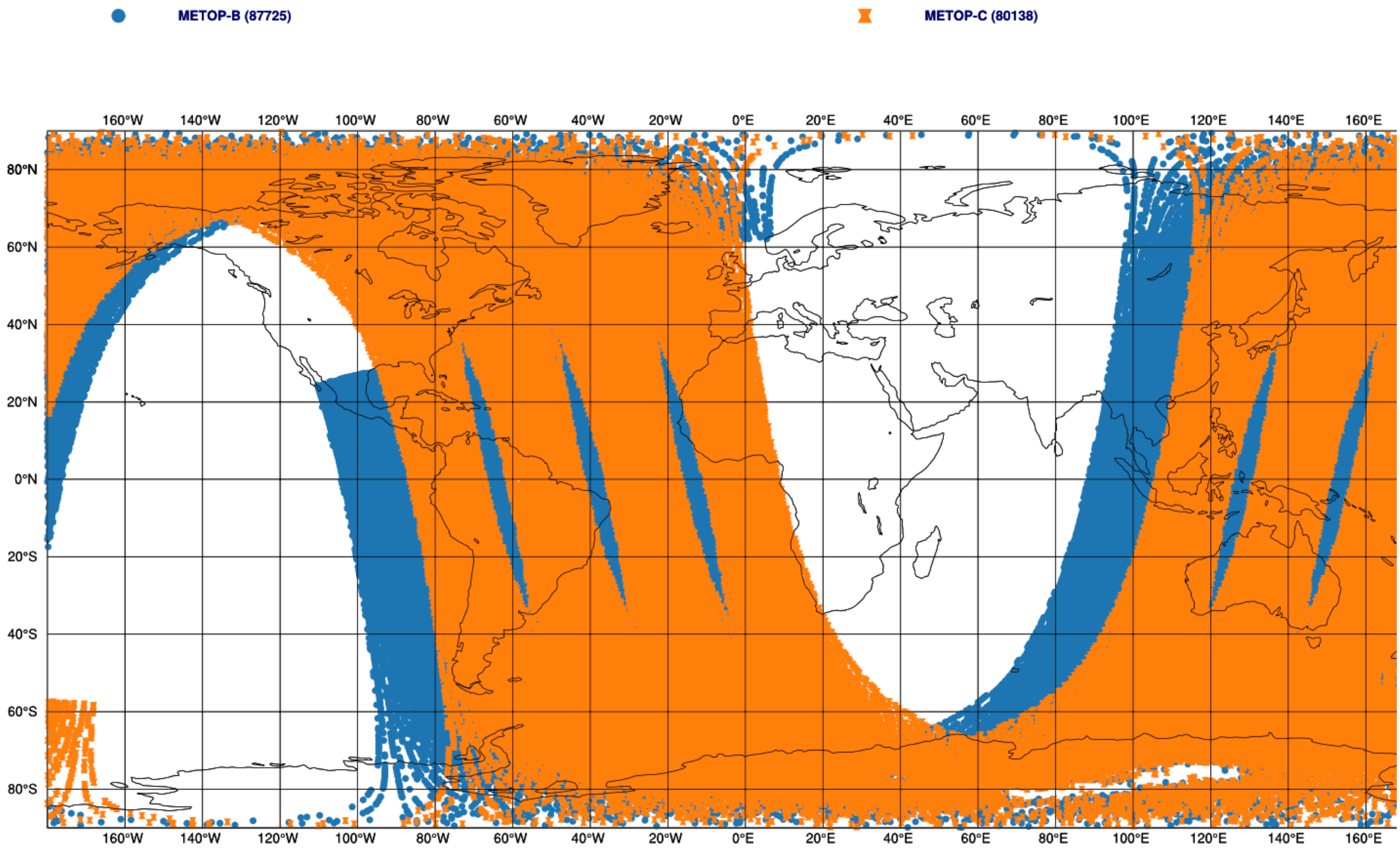

ECMWF data coverage (all observations) - AMV WV
2025040921 to 2025041003
Total number of obs = 3566525

METEOSAT-9 (147431) TERRA (2196) AQUA (1567) METEOSAT-10 (145735)

FY-2G (33718) METEOSAT-11 (85537) HIMAWARI-9 (219673) METEOSAT (2189041)

GEO-KOMPSAT-2A (741627)

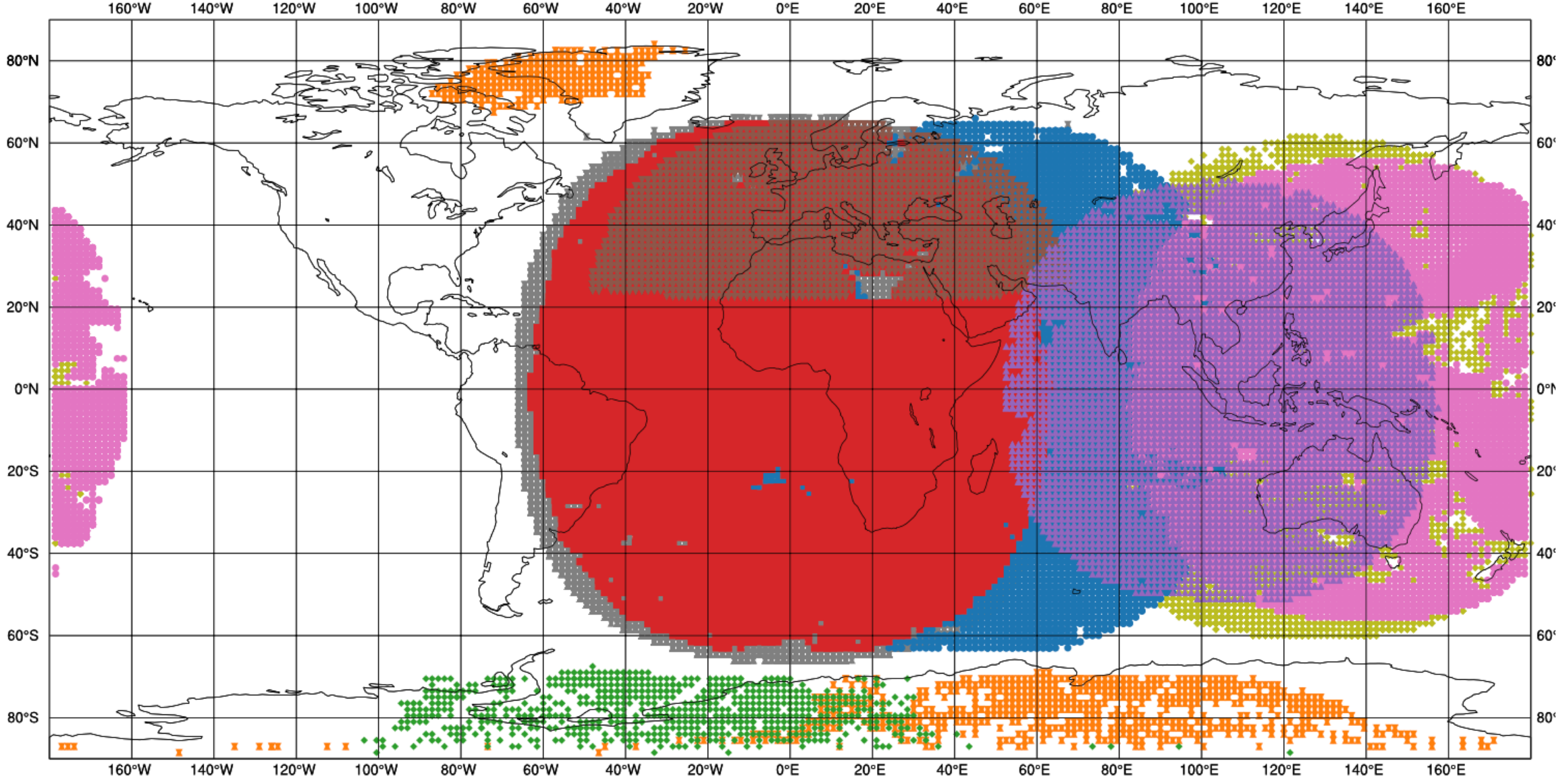

ECMWF data coverage (all observations) - AMV VIS
2025040921 to 2025041003
Total number of obs = 613632

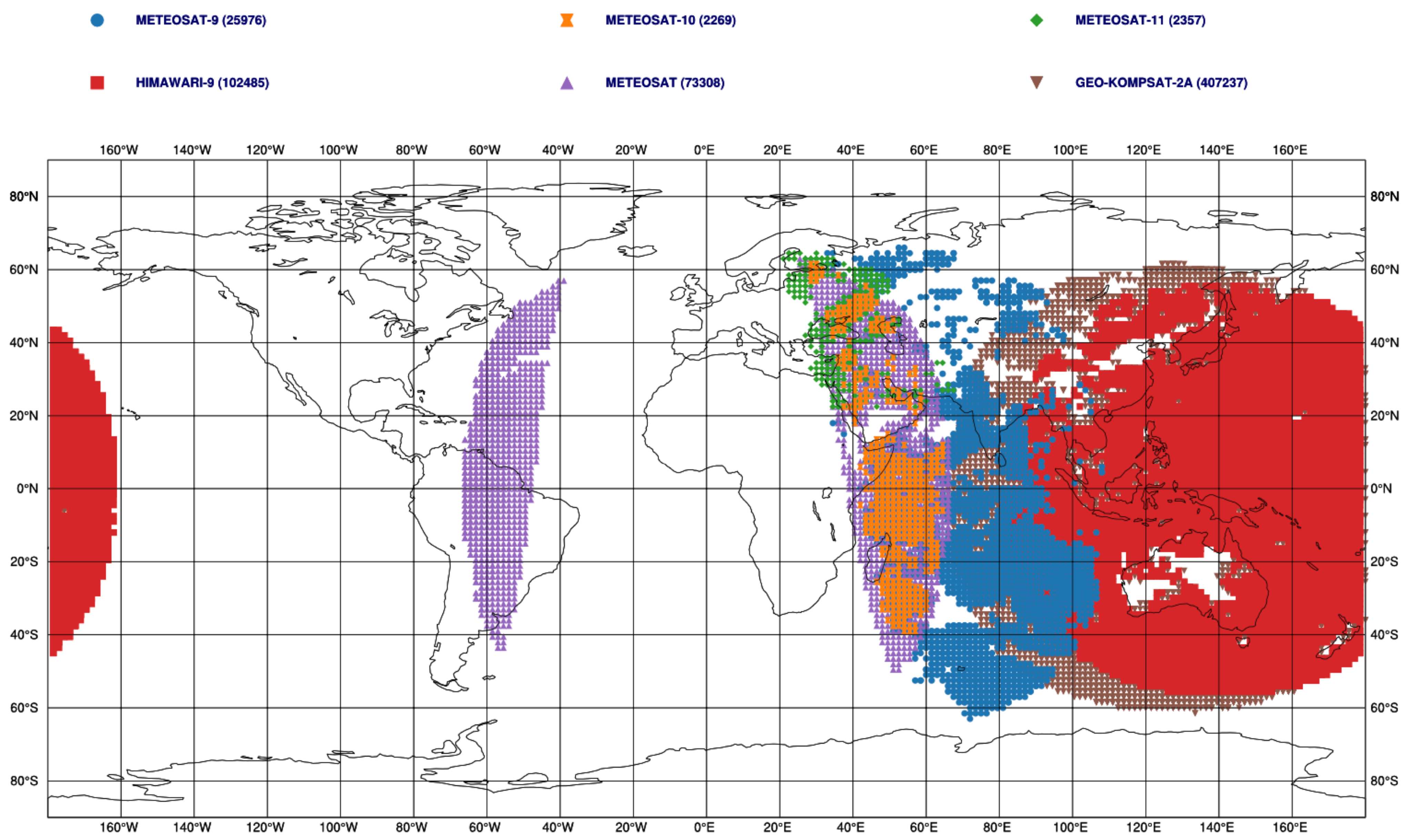

ECMWF data coverage (all observations) - GPSRO
2025040921 to 2025041003
Total number of obs = 67617

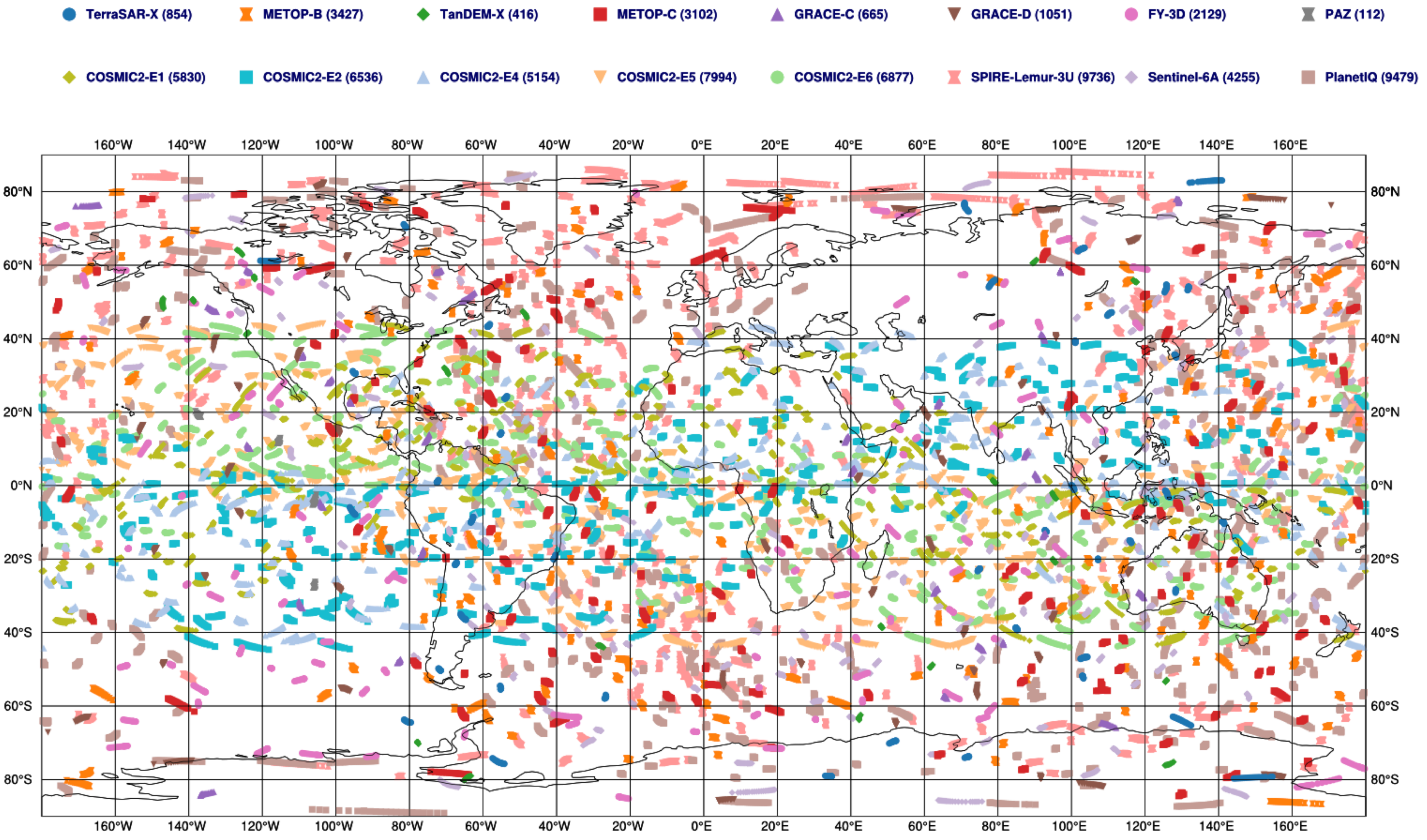

ECMWF

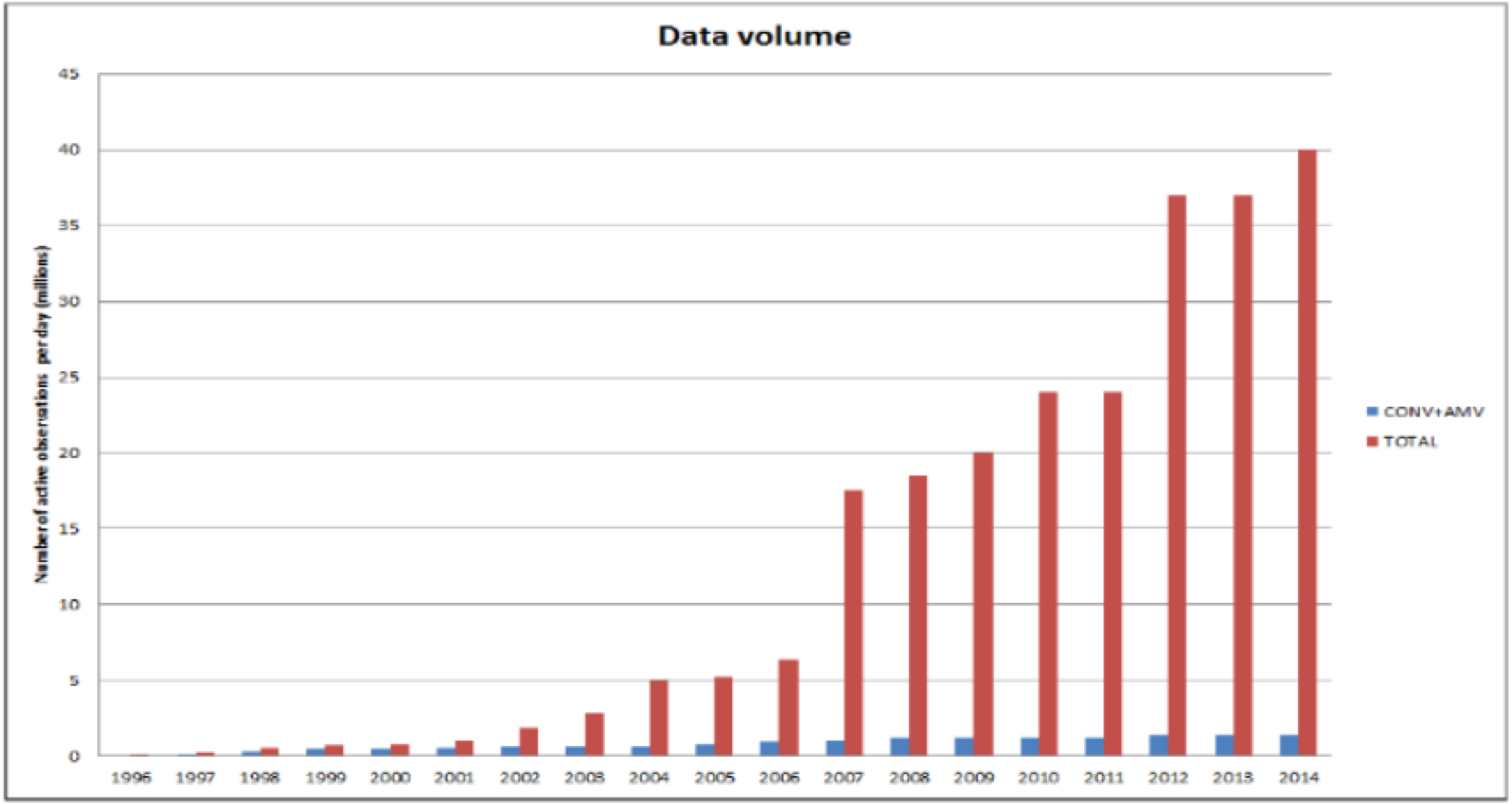

Amount of 40 million scalar data used over each 24-hour period still valid as of 2025

- *Synoptic* observations (ground observations, radiosonde observations), performed simultaneously, by international agreement, in all meteorological stations around the world (00:00, 06:00, 12:00, 18:00 UTC)

- *Asynoptic* observations (satellites, aircraft), performed more or less continuously in time.

- *Direct* observations (temperature, pressure, horizontal components of the wind, moisture), which are local and bear on the variables used for describing the flow in numerical models.

- *Indirect* observations (radiometric observations, …), which bear on some more or less complex combination (most often, a one-dimensional spatial integral) of variables used for for describing the flow

$$y = H(\boldsymbol{x})$$

H : *observation operator (*for instance, radiative transfer equation)

ECMWF data coverage (all observations) - SEA LEVEL ANOMALY

20250408 00

Total number of obs = 9268

CRYOSAT-2 (2221)

SARAL (2474)

Sentinel-3A (2249)

Sentinel-3B (2324)

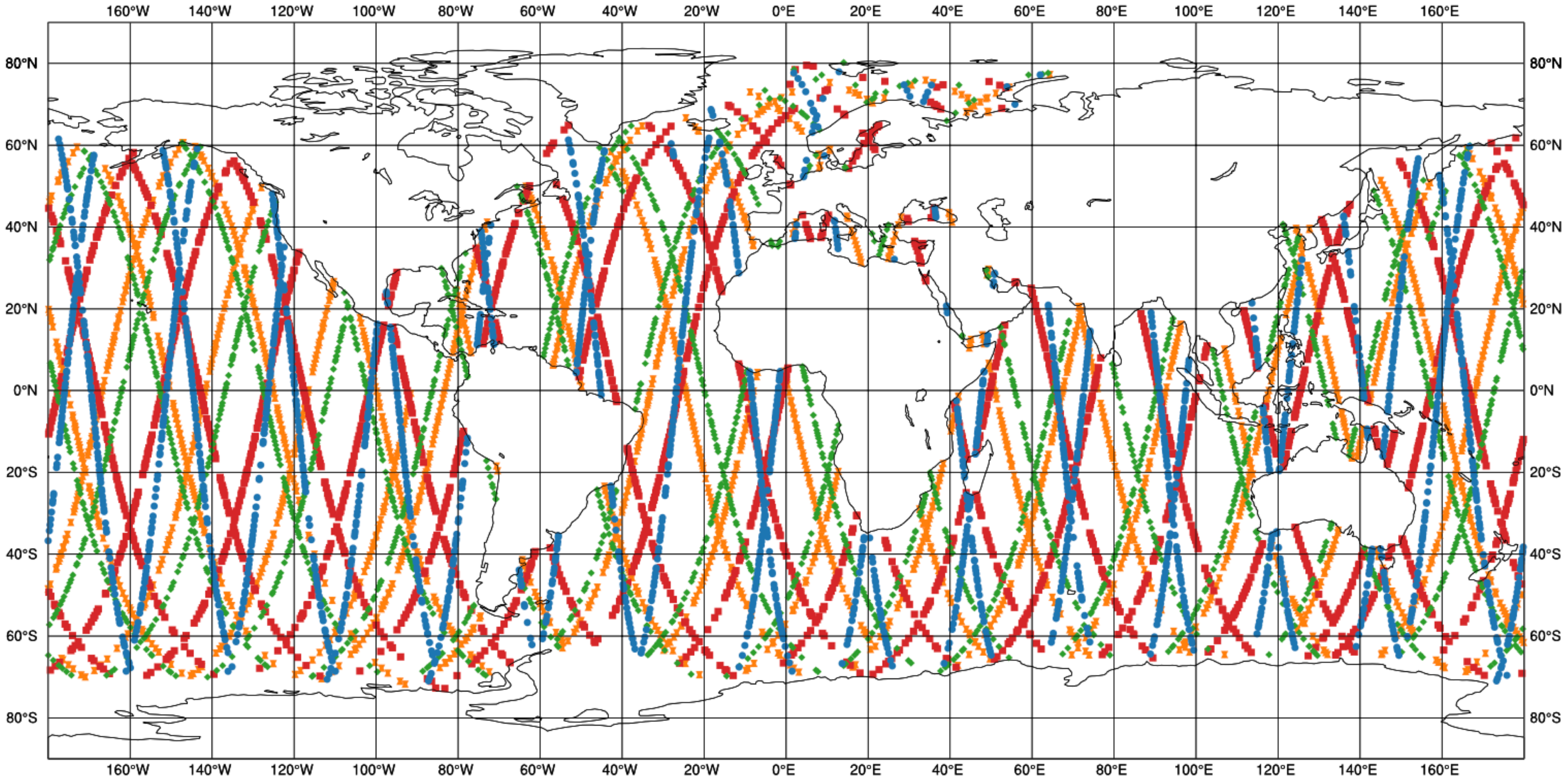

ARGO Programme

International programme for observation of the ocean. Has been in operation for 20 years. 4000 floaters drift at about 1000-m depth, measuring temperature, pressure and biochemical parameters. Drifters come to the surface every 10 days or so, and send their data, including profiles, to satellites.

US Argo Profile Locations Observed in the Last 12 Days
World Ocean
Apr 06, 2025

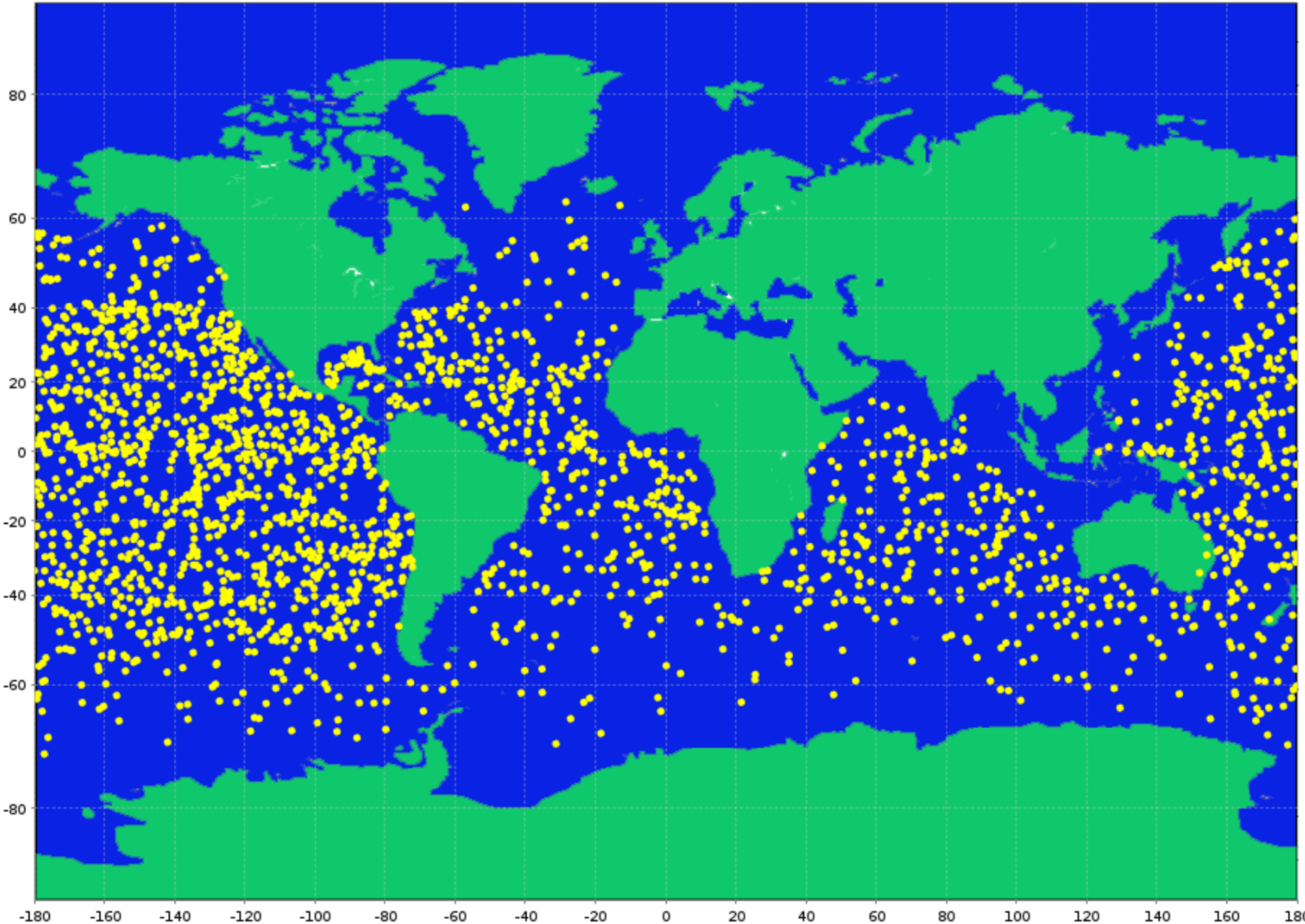

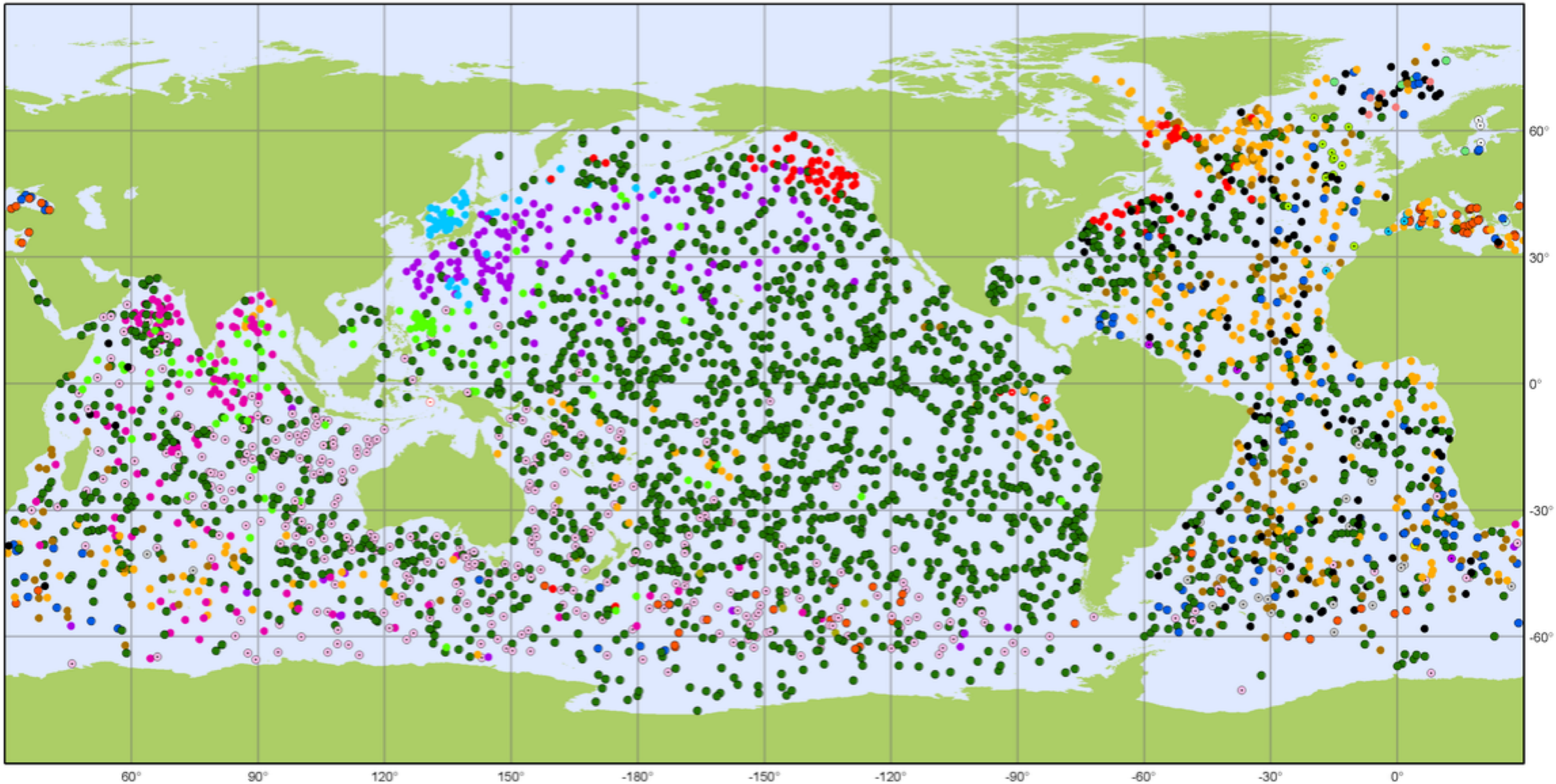

Argo **National contributions - 3881 Operational Floats** **February 2018**

Latest location of operational floats (data distributed within the last 30 days)

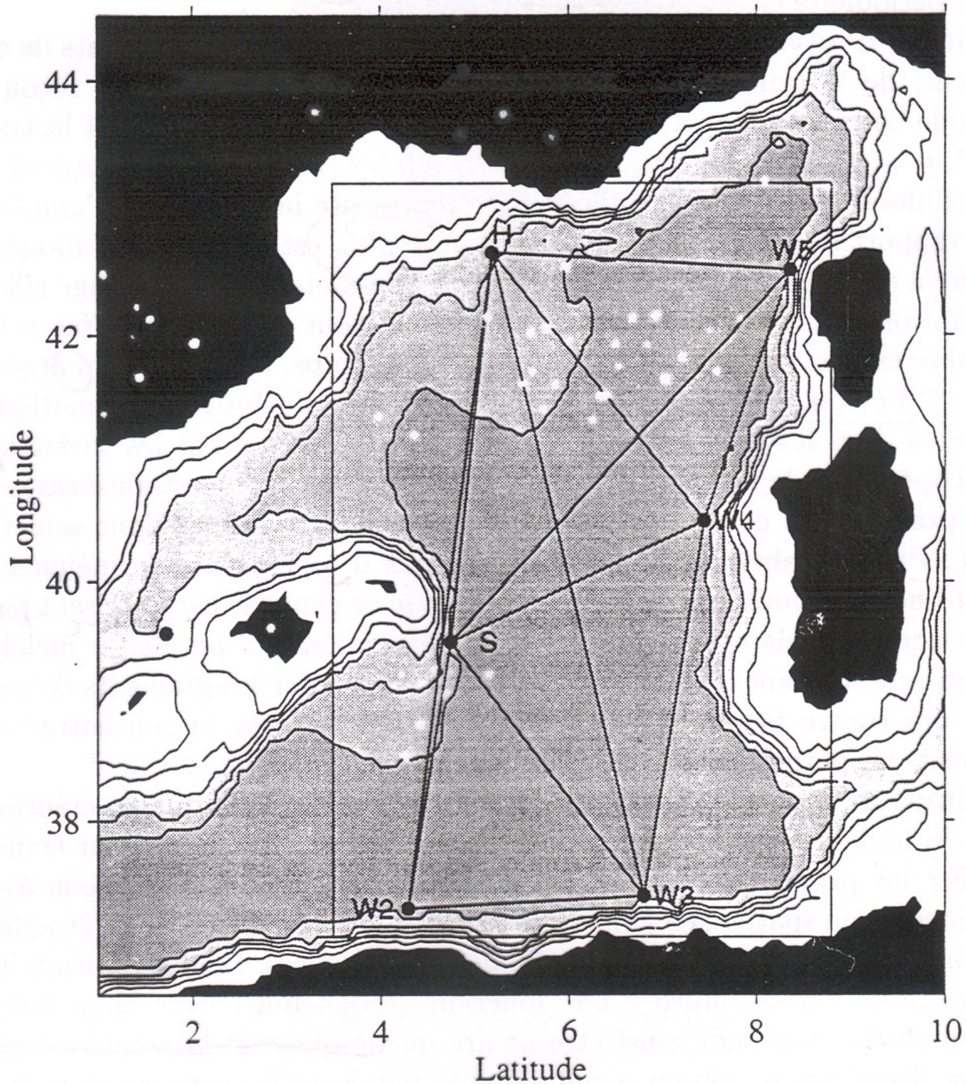

FIG. 1 – *Bassin méditerranéen occidental: réseau d'observation tomographique de l'expérience Thétis 2 et limites du domaine spatial utilisé pour les expériences numériques d'assimilation.*

E. Rémy, Doctoral Dissertation, 1999

Purpose of assimilation : reconstruct as accurately as possible the state of the atmospheric or oceanic flow, using all available appropriate information. The latter essentially consists of

- The observations proper, which vary in nature, resolution and accuracy, and are distributed more or less regularly in space and time.

- The physical laws governing the evolution of the flow, available in practice in the form of a discretized, and necessarily approximate, numerical model.

- 'Asymptotic' properties of the flow, such as, *e. g.*, geostrophic balance of middle latitudes. Although they basically are necessary consequences of the physical laws which govern the flow, these properties can usefully be explicitly introduced in the assimilation process.

Both observations and 'model' are affected with some uncertainty $\Rightarrow$ uncertainty on the estimate.

For some reason, uncertainty is conveniently described by probability distributions (don't know too well why, but it works; see, *e.g*. Jaynes, 2007, *Probability Theory: The Logic of Science,* Cambridge University Press).

Assimilation is a problem in bayesian estimation.

Determine the conditional probability distribution for the state of the system, knowing everything we know (see Tarantola, A., 2005*, Inverse Problem Theory and Methods for Model Parameter Estimation*, SIAM).

Assimilation is one of many '*inverse problems*' encountered in many fields of science and technology

- solid Earth geophysics
- plasma physics
- 'nondestructive' probing
- navigation (spacecraft, aircraft, ….)
- …

Solution most often (if not always) based on Bayesian, or probabilistic, estimation. 'Equations' are fundamentally the same.

Difficulties specific to assimilation of meteorological observations :

- Very large numerical dimensions ($n \approx 10^6$-10^9 parameters to be estimated, $p \approx$ 4-5.10^7 observations per 24-hour period). Difficulty aggravated in Numerical Weather Prediction by the need for the forecast to be ready in time.

- Non-trivial, actually chaotic, underlying dynamics

HPC SBU Usage during current ISO 8601 Year: 2022

Medium-range forecast (ENS): 30.66%

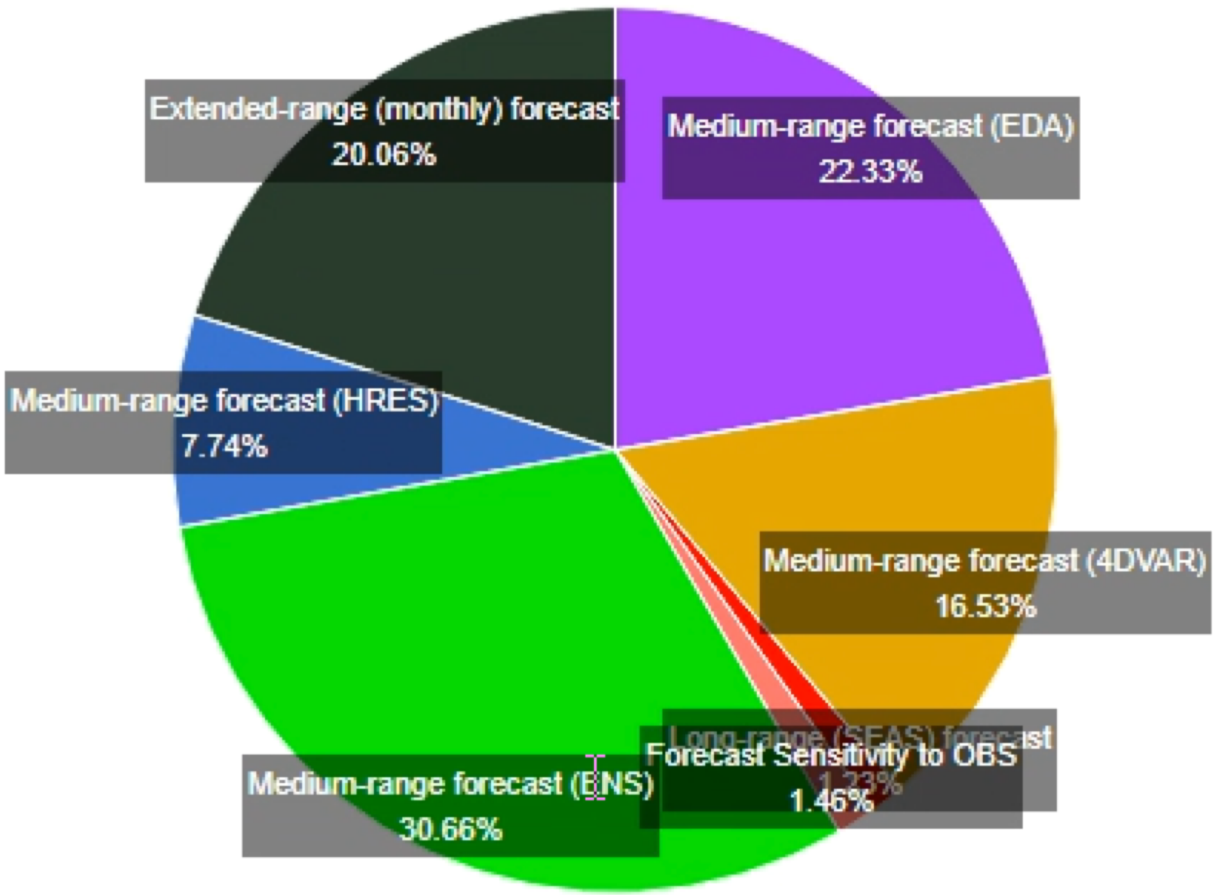

Courtesy J.-N. Thépaut (ECMWF)

Gaussian variables

Unidimensional

$$\mathcal{N}[m,\, a] \;\sim (2\pi\, a)^{-1/2} \exp\,[-\,(1/2a)\,(\xi\text{-}m)^2]$$

Dimension n

$$\mathcal{N}[\boldsymbol{m},\, \boldsymbol{A}] \sim$$
$$[(2\pi)^n\, \det\boldsymbol{A}]^{-1/2} \exp\,[-\,(1/2)\,(\boldsymbol{\xi}\text{-}\boldsymbol{m})^{\mathrm{T}}\boldsymbol{A}^{-1}(\boldsymbol{\xi}\text{-}\boldsymbol{m})]$$

Bayesian Estimation. A simple example

Determine conditional probability distribution of the state of the system, given the probability distribution of the uncertainty on the data

$z_1 = x + \zeta_1$ $\qquad$ $\zeta_1 = \mathcal{N}[0, s_1]$

density function $p_1(\zeta) \propto \exp[\,-(\zeta^2)/2s_1]$

$z_2 = x + \zeta_2$ $\qquad$ $\zeta_2 = \mathcal{N}[0, s_2]$

density function $p_2(\zeta) \propto \exp[\,-(\zeta^2)/2s_2]$

ζ_1 and ζ_2 mutually independent

What is the conditional probability $P(x = \xi \mid z_1, z_2)$ that x be equal to some value ξ ?

$z_1 = x + \zeta_1$ density function $p_1(\zeta) \propto \exp[-(\zeta^2)/2s_1]$

$z_2 = x + \zeta_2$ density function $p_2(\zeta) \propto \exp[-(\zeta^2)/2s_2]$

ζ_1 and ζ_2 mutually independent

$x = \xi \Leftrightarrow \zeta_1 = z_1 - \xi$ and $\zeta_2 = z_2 - \xi$

$$P(x = \xi \mid z_1, z_2) \propto p_1(z_1 - \xi)\, p_2(z_2 - \xi)$$

$$\propto \exp[-(\xi - x^a)^2/2p^a]$$

where $1/p^a = 1/s_1 + 1/s_2$, $x^a = p^a (z_1/s_1 + z_2/s_2)$

Conditional probability distribution of x, given z_1 and z_2 : $\mathcal{N}[x^a, p^a]$

$p^a < (s_1, s_2)$ independent of z_1 and z_2

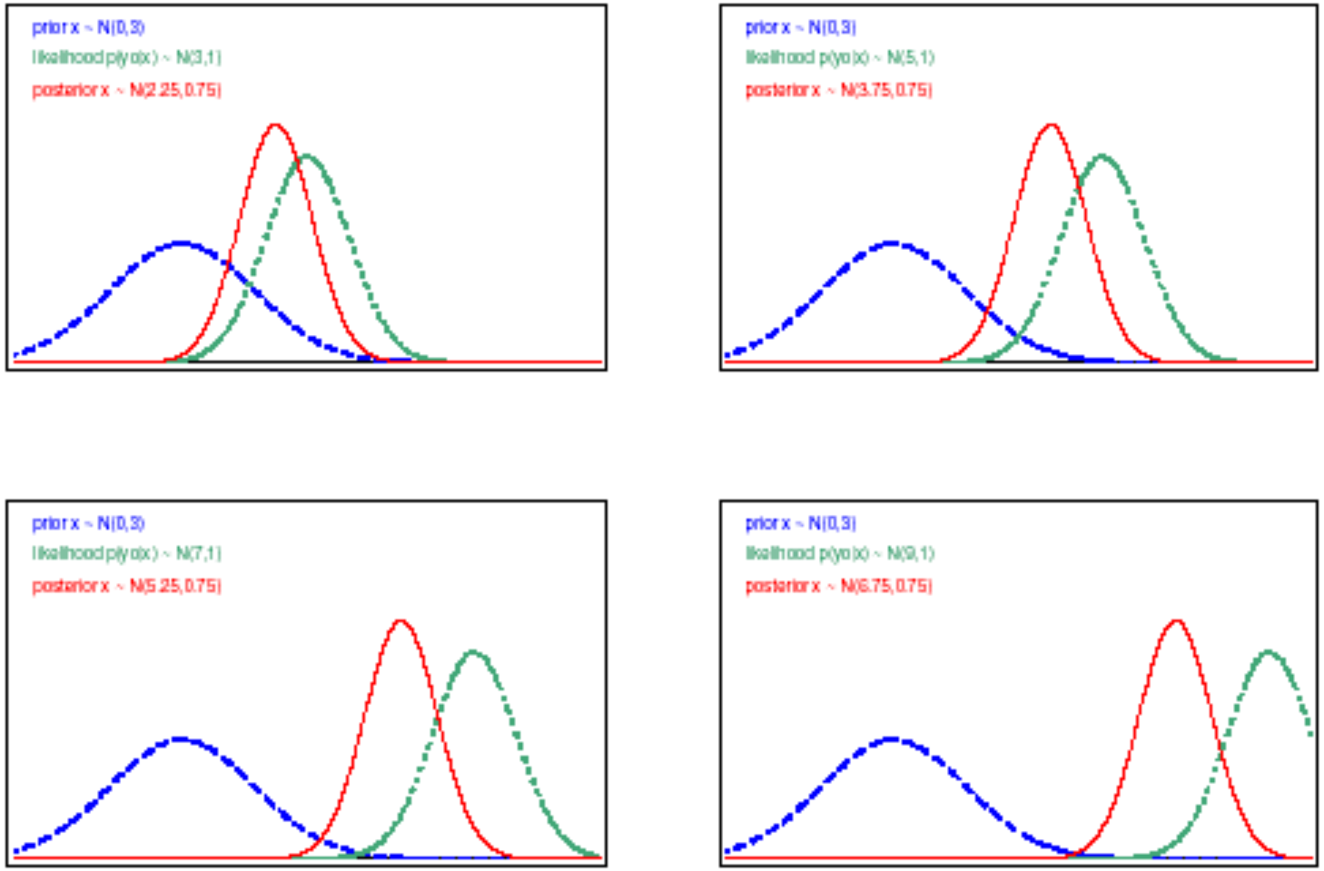

Fig. 1.1: Prior pdf $p(x)$ (dashed line), posterior pdf $p(x|y^o)$ (solid line), and Gaussian likelihood of observation $p(y^o|x)$ (dotted line), plotted against x for various values of y^o. (Adapted from Lorenc and Hammon 1988.)

Conditional expectation x^a minimizes following scalar *objective function*, defined on ξ-space

$$\xi \rightarrow \mathcal{J}(\xi) \equiv (1/2)\,[(z_1 - \xi)^2 / s_1 + (z_2 - \xi)^2 / s_2\,]$$

In addition

$$p^a = 1/\,\mathcal{J}''(x^a)$$

Conditional probability distribution in Gaussian case

$$P(x = \xi \mid z_1, z_2) \propto \exp[\, - \underbrace{(\xi - x^a)^2/2p^a}_{\mathcal{J}(\xi)\,+\,Cst}]$$

Estimate

$$x^a = p^a\,(z_1/s_1 + z_2/s_2)$$

with error p^a such that

$$1/p^a = 1/s_1 + 1/s_2$$

can also be obtained, independently of any Gaussian hypothesis, as simply corresponding to the linear combination of z_1 and z_2 that minimizes the error $E\,[(x^a - x)^2]$

Best Linear Unbiased Estimator (*BLUE*)

$z_1 = x + \zeta_1$
$z_2 = x + \zeta_2$

Same as before, but ζ_1 and ζ_2 are now distributed according to exponential law with parameter a, *i. e.*

$$p(\zeta) \propto \exp[-|\zeta|/a] \quad ; \quad \mathrm{Var}(\zeta) = 2a^2$$

Conditional probability density function is now uniform over interval $[z_1, z_2]$, exponential with parameter $a/2$ outside that interval

$$E(x \mid z_1, z_2) = (z_1+z_2)/2$$

$\mathrm{Var}(x \mid z_1, z_2) = a^2\,(2\delta^3/3 + \delta^2 + \delta + 1/2) \,/\, (1 + 2\delta)$, with $\delta = |z_1 - z_2|/(2a)$

Increases from $a^2/2$ to ∞ as δ increases from 0 to ∞. Can be larger than variance $2a^2$ of original errors (probability 0.08)

Bayesian estimation

State vector $\boldsymbol{x}$, belonging to *state space* $\mathcal{S}$ ($\dim \mathcal{S} = n$), to be estimated.

Data vector $\boldsymbol{z}$, belonging to *data space* $\mathcal{D}$ ($\dim \mathcal{D} = m$), available.

$$z = F(\boldsymbol{x}, \zeta) \qquad (1)$$

where ζ is a random element representing the uncertainty on the data (or, more precisely, on the link between the data and the unknown state vector).

For example

$$\boldsymbol{z} = \boldsymbol{\Gamma x} + \zeta$$

Bayesian estimation (continued)

Probability that $\boldsymbol{x} = \xi$ for given ξ ?

$$\boldsymbol{x} = \xi \quad \Rightarrow \quad z = F(\xi, \zeta)$$

$$P(\boldsymbol{x} = \xi \mid z) = P[z = F(\xi, \zeta)] \;/\; \int_{\xi'} P[z = F(\xi', \zeta)]$$

Unambiguously defined iff, for any ζ, there is at most one $\boldsymbol{x}$ such that (1) is verified.

$\Leftrightarrow$ data contain information, either directly or indirectly, on any component of $\boldsymbol{x}$. *Determinacy* condition. Implies $m \geq n$.

Bayesian estimation is actually impossible in its general theoretical form in meteorological or oceanographical practice because

- It is impossible to explicitly describe a probability distribution in a space with dimension even as low as $n \approx 10^3$, not to speak of the dimension $n \approx 10^{6\text{-}9}$ of present Numerical Weather Prediction models (the *curse of dimensionality)*.

- Probability distribution of errors on data very poorly known (model errors in particular).

One has to restrict oneself to a much more modest goal. Two approaches exist at present

- Obtain some 'central' estimate of the conditional probability distribution (expectation, mode, …), plus some estimate of the corresponding spread (standard deviations and a number of correlations).

- Produce an ensemble of estimates which are meant to sample the conditional probability distribution (dimension $N \approx O(10\text{-}100)$).

Cours à venir

Mercredi 2 avril

Vendredi 11 avril

Vendredi 18 avril

Mercredi 23 avril

Lundi 12 mai

Mercredi 28 mai

Mercredi 11 juin

Mercredi 18 juin

- Reminder on elementary probability theory. Random vectors and covariance matrices, random functions and covariance functions

- *Optimal Interpolation*. Principle, simple examples, basic properties.

- *Best Linear Unbiased Estimate* (*BLUE*)